I. Clusters of galaxies and large scale structure

I. Aretxaga

A bit of history

- Charles Messier published his famous catalogue of nebulae in 1784.
- He noted that: “The constellation of Virgo… is one of the constellations that contains the greatest number of nebulae”
- Other similar concentrations of nebulae were found in the 18th and 19th centuries by the Herschels.
- William Herschel (1785) commented on: “That remarkable collection of many hundreds of nebulae which can be seen in what I call the nebulous startum of Coma Berenices”
- Other clusters of nebulae were discovered by: Wolf (1902, 1906), Lundmark (1927), Baade (1928), Christie (1929), Hubble and Humason (1931), Shapley (1934)

Why study clusters of galaxies?

- Clusters are the largest objects in the universe to have reached a quasi-equilibrium state.
- Clusters provide excellent laboratories to study galaxy formation, evolution and interactions.
- Clusters provided the first and best evidence of vast quantities of dark matter in the universe.
- Clusters have provided important insights into a wide range of topics, such as high-energy astrophysics, particle physics, cosmology, etc…
- Clusters can be used to map the large-scale structure of the universe

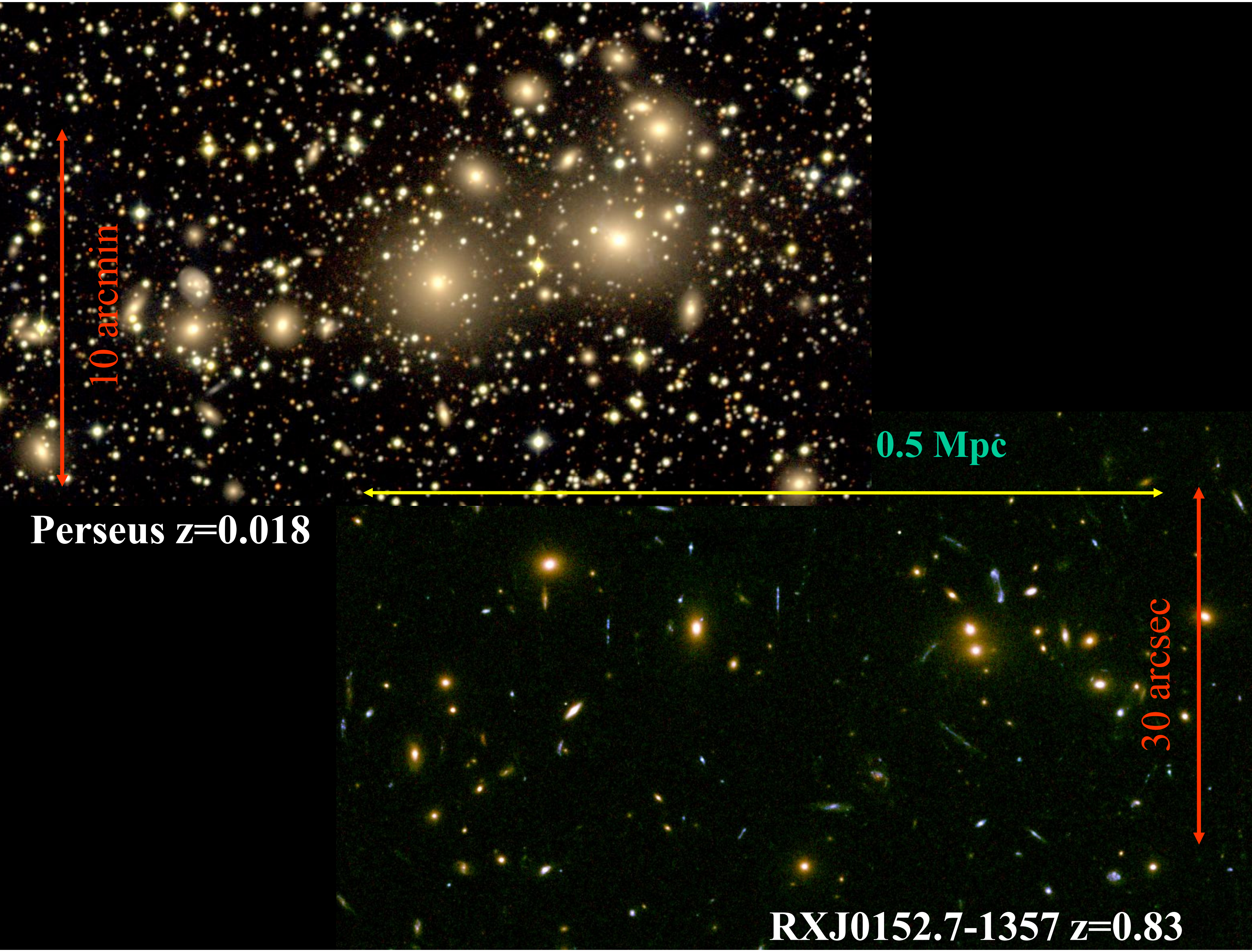
10 arcmin
0.5 Mpc
Perseus z=0.018
30 arcsec
RXJ0152.7-1357 z=0.83

The Coma Cluster

Only 10% of the mass is visible (gas and stars)

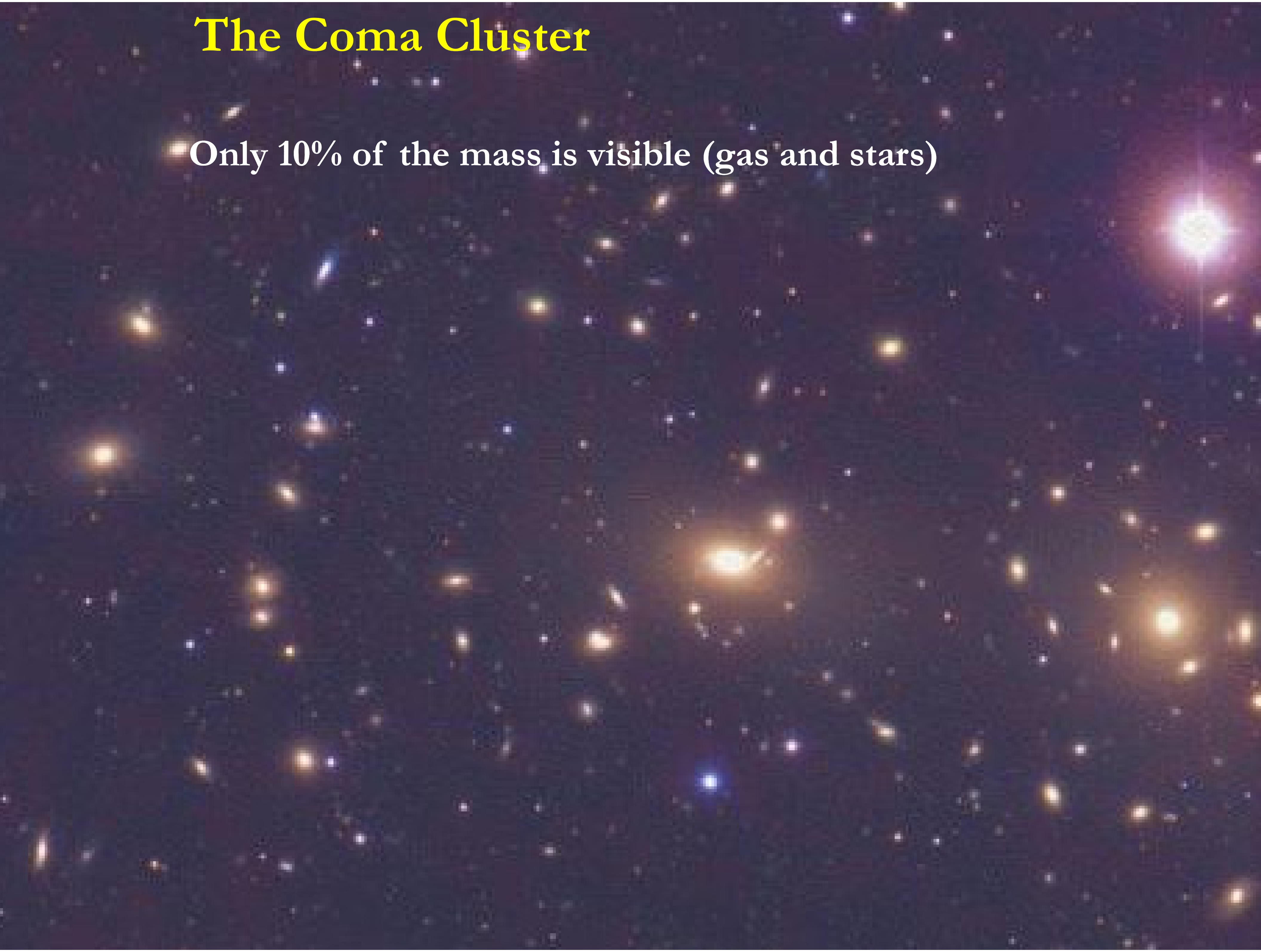

The CfA Slice

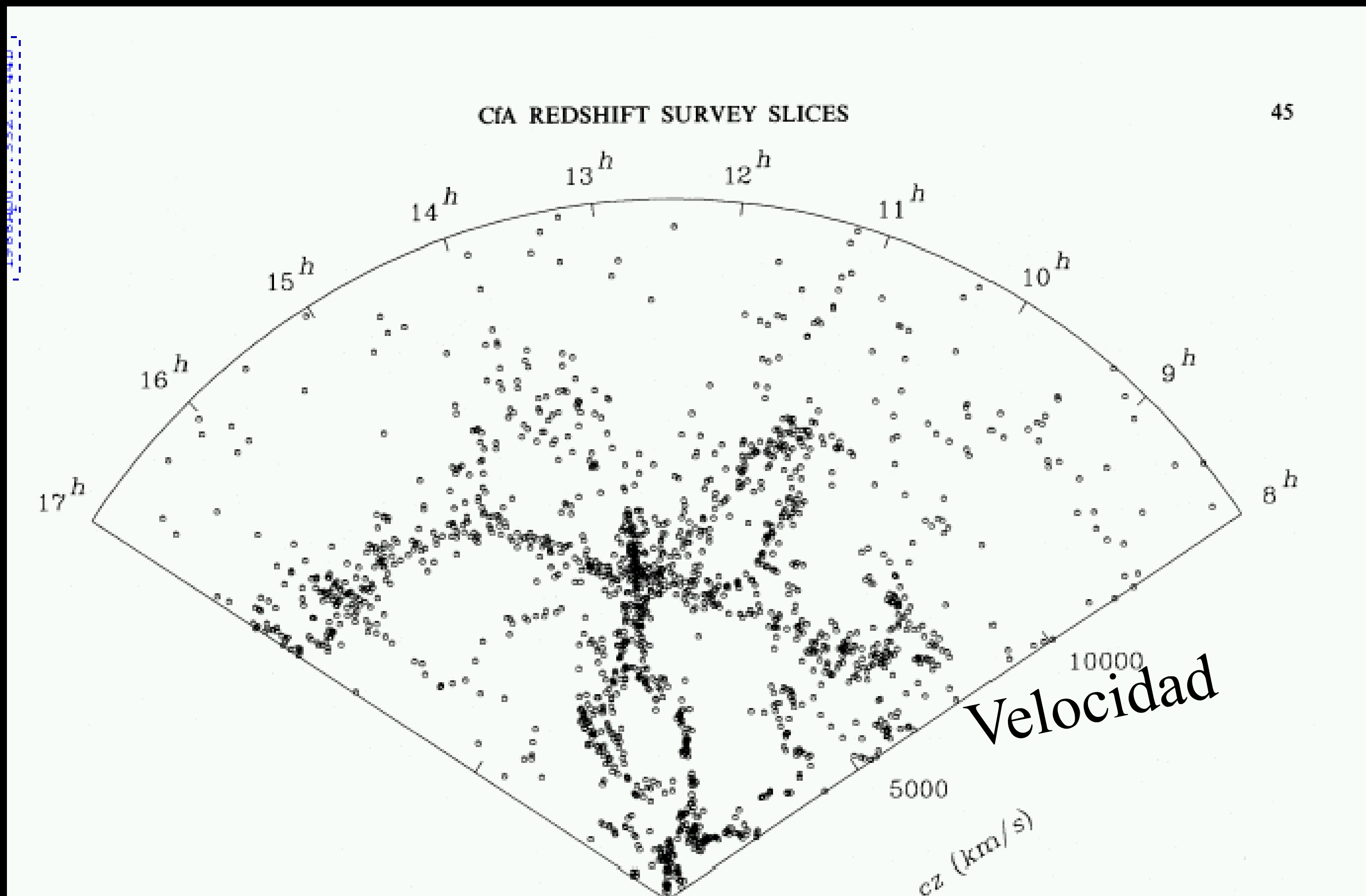

Fig. 1.—Map of the galaxy distribution in right ascension and velocity in the 12° strip limited by $m_{B(0)} \leq 15.5$. The declination range is $26.^\circ5 \leq \delta \geq 38.^\circ5$. This map contains 1761 galaxies.

Ley de Hubble

$d = v/H_0$

De Lapparent et al. 1988

Large scale structure – 2dF

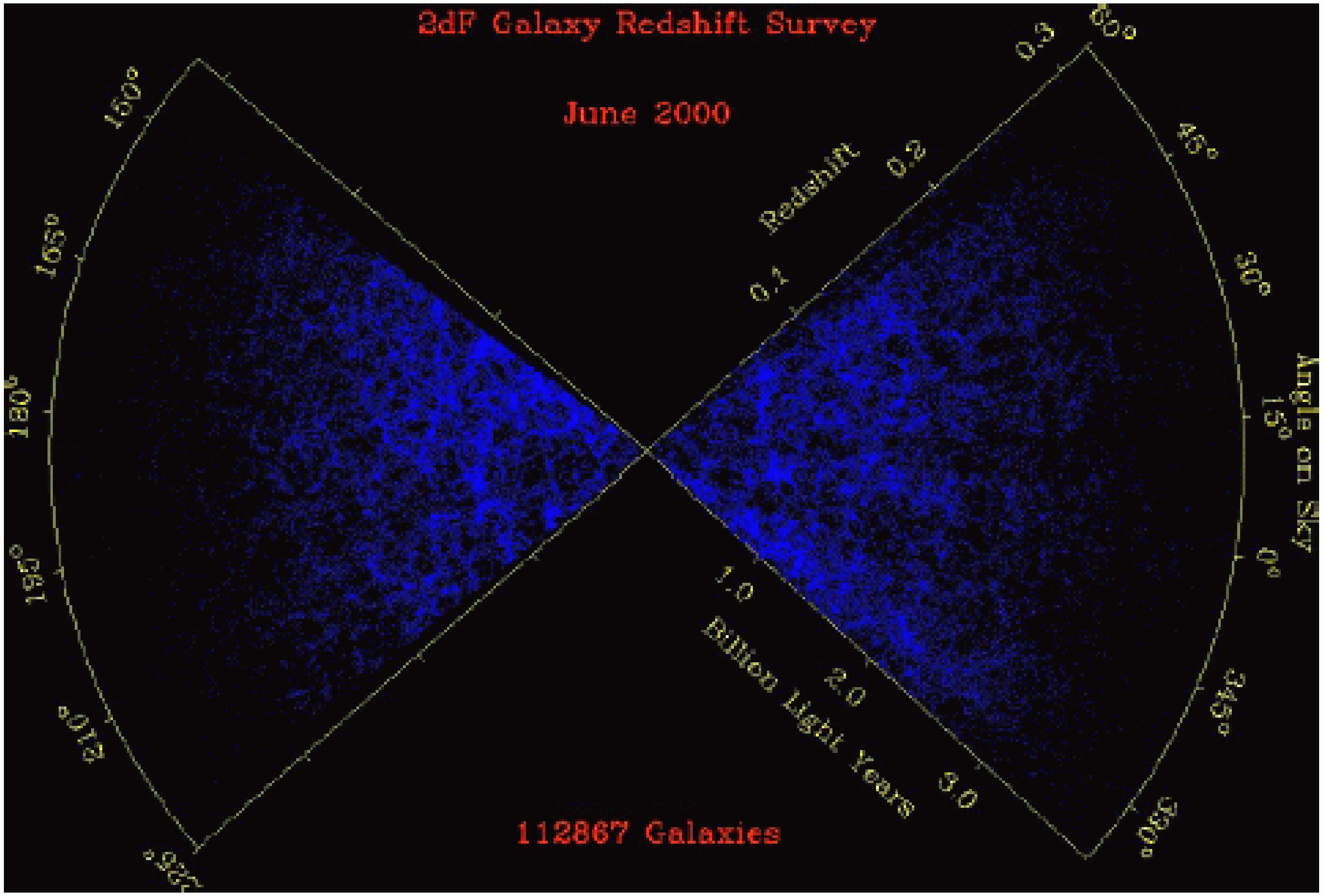

2dF Galaxy Redshift Survey

Model – lambda cold dark matter

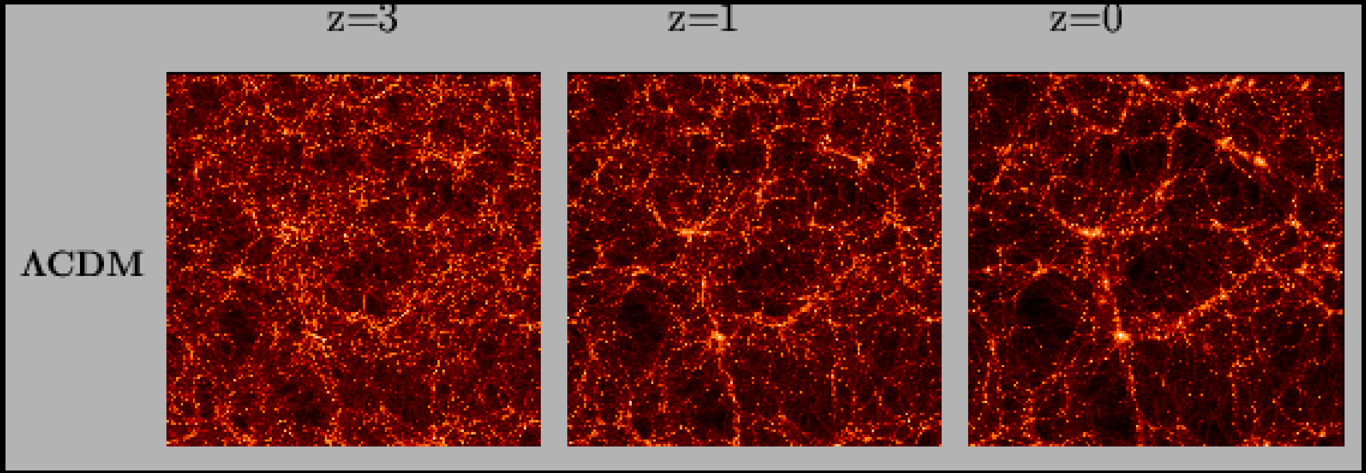

This image shows the hierarchical clustering in computer Simulation for ΛCDM models. The smallest structures visible are clusters. Clusters are still forming today! Many of them may therefore not be virialized.

Very important

- Galaxy clustering is a continuous hierarchy
- Any attempt to identify individual clusters requires rather arbitrary and subjective boundaries to be drawn.
- There is no unique and unambiguous definition of what constitutes a cluster of galaxies, and thus no single method of identifying them.
- For this reason, studies of clusters and their properties depend on the methods used to identify and catalogue them.

The Virgo cluster

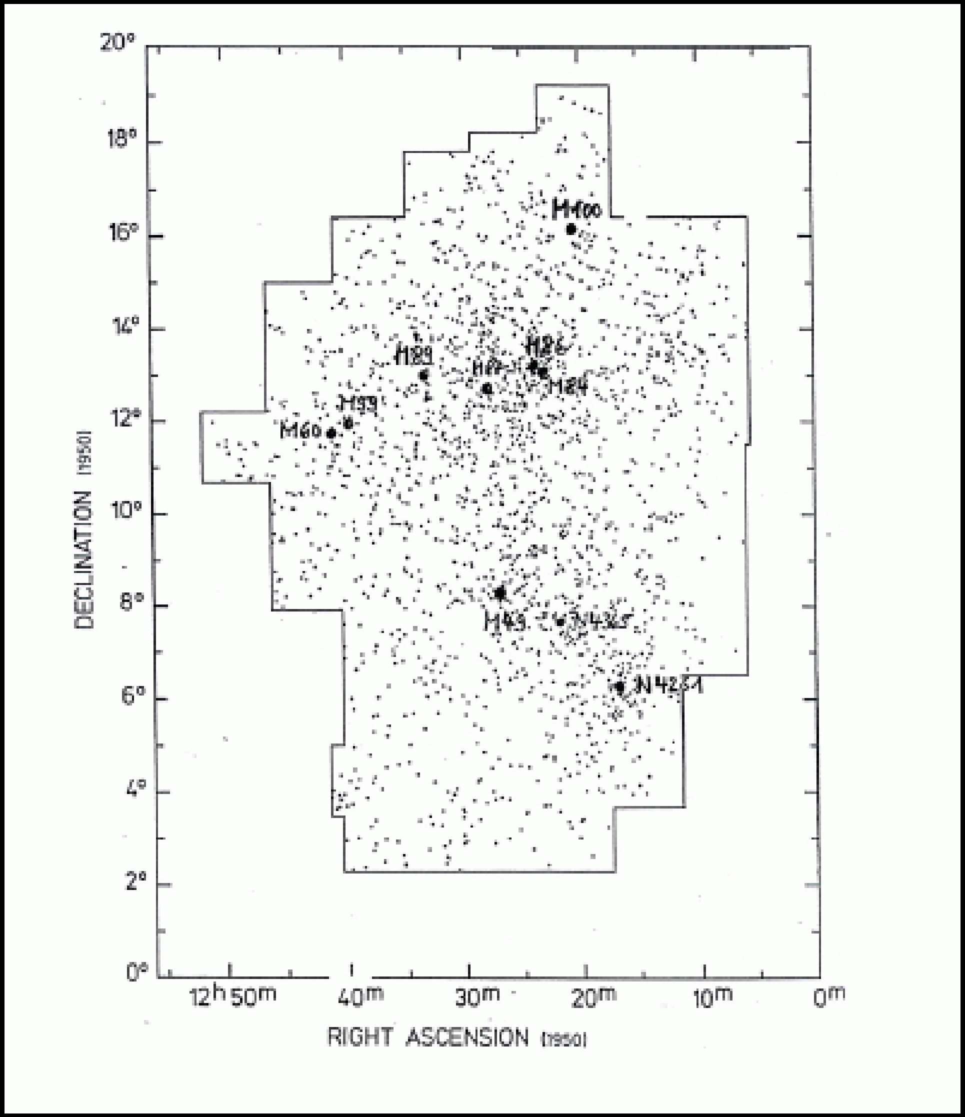

It is 15 Mpc from Earth

It has several thousand galaxies

70% of galaxies are spirals

The distribution of galaxies is clumpy

The LG is infalling towards Virgo

The Virgo cluster

The Coma cluster

Distance: 70 Mpc (z=0.02)

Brightest members are ellipticals

~ up to 10000 members

Best-studied of all clusters

The Coma cluster

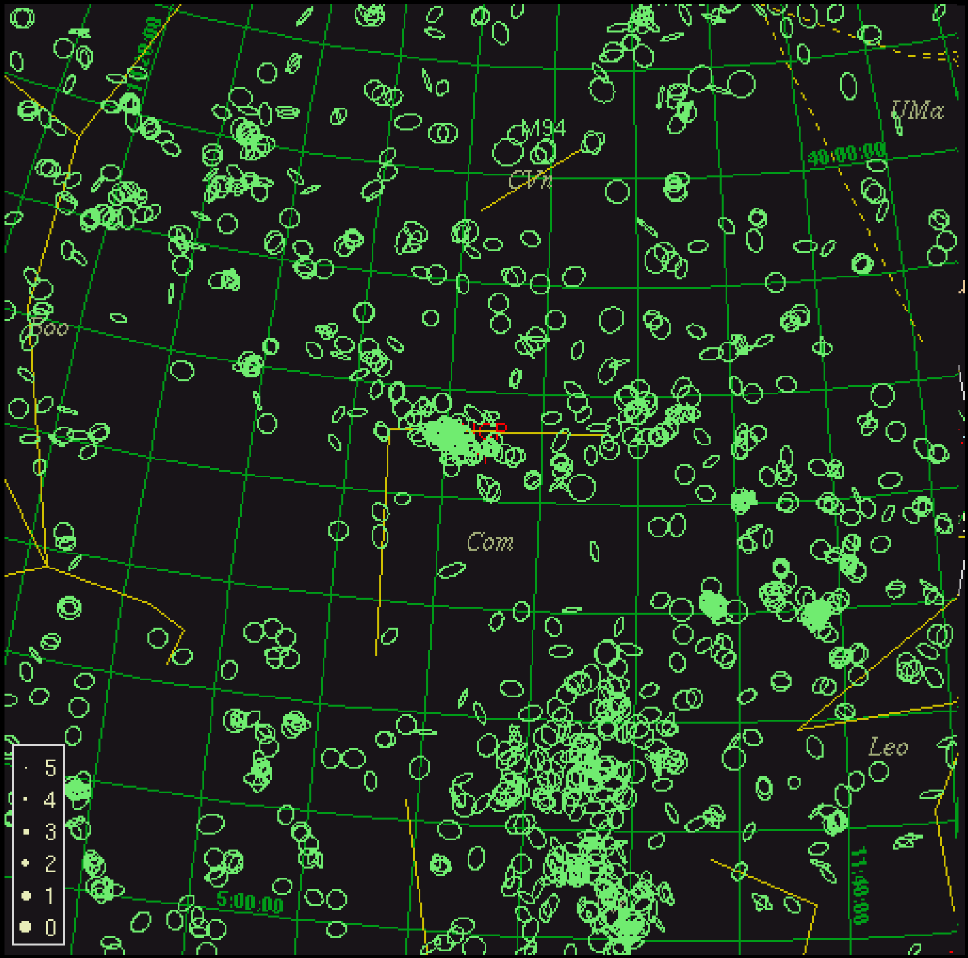

Cluster catalogues

19.1 Selection Criteria for Clusters and Groups

19.1.1 Abell's Catalog of Rich Clusters (1958)

Abell's criteria:

- > 50 cluster members in the magnitude range $[m_3, m_3 + 2]$ (with the magnitude m_3 of the 3rd brightest galaxy) and within the radius $R_{\text{Abell}} = \frac{1.7}{(1+z)} \simeq 3 h_{50} Mpc$.
- Redshift range: $0.02 < z < 0.20$
- Sorted into 'richness classes' according to number of galaxies N and density.
- The redshift was usually not measured, but determined from the apparent magnitude of the brightest cluster galaxies.
- The clusters were found using the Palomar Sky Survey

Richness class R	N	Number of clusters in the complete northern sample
0	$30 - 49$	$\geq 10^3$
1	$50 - 79$	1224
2	$80 - 129$	383
3	$130 - 199$	68
4	$200 - 299$	6
5	≥ 300	1

Zwicky et al. (1961-1968)

- Zwicky catalogued about 10000 clusters by eye
- Because a less rigorous cluster definition was used, this catalogue is not as complete or homogeneous as Abell's

Shectman (1985)

An automated computer procedure was used to identify 646 clusters from the Lick galaxy survey

Edinburgh-Durham Cluster Catalog (Lumsden et al. 1992)

- An automated procedure based on Abell's cluster definition was used
- 737 clusters were identified in the southern sky

APM Cluster Catalog (Dalton et al. 1992)

A different automated procedure was used

Galaxies were counted within r=0.075 h-1 Mpc

Different magnitude range

220 clusters were cataloued

2dF and SDSS cluster surveys - several

X-ray galaxy cluster surveys

- BCS, XBCS, REFLEX, EMSS, PSPC
- SHARC, WARPS, MACS

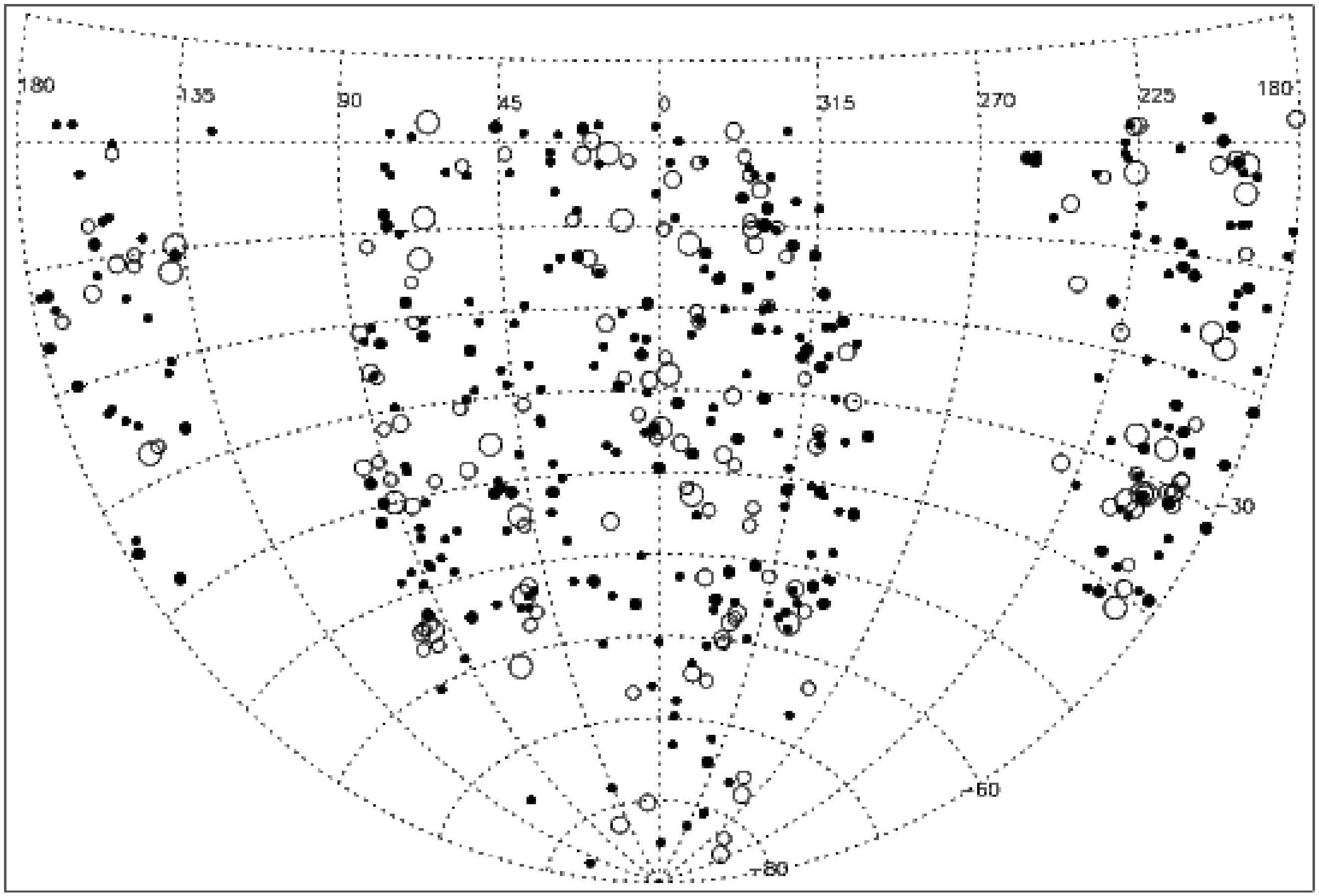

Fig. 1. Sky distribution in α and δ of the galaxy clusters in the REFLEX sample. The symbols give an indication of the cluster flux. The clusters are sorted into five flux bins: $3-5\cdot10^{-12}$, $5-7\cdot10^{-12}$, $7-10\cdot10^{-12}$, $1-2\cdot10^{-11}$, and $\geq 2\cdot10^{-11}$ erg s^{-1} cm^{-2} and indicated by increasing symbol size, respectively. The three largest symbol classes are shown as open circles to avoid shading of other clusters.

Flux limits of X-ray cluster catalogues

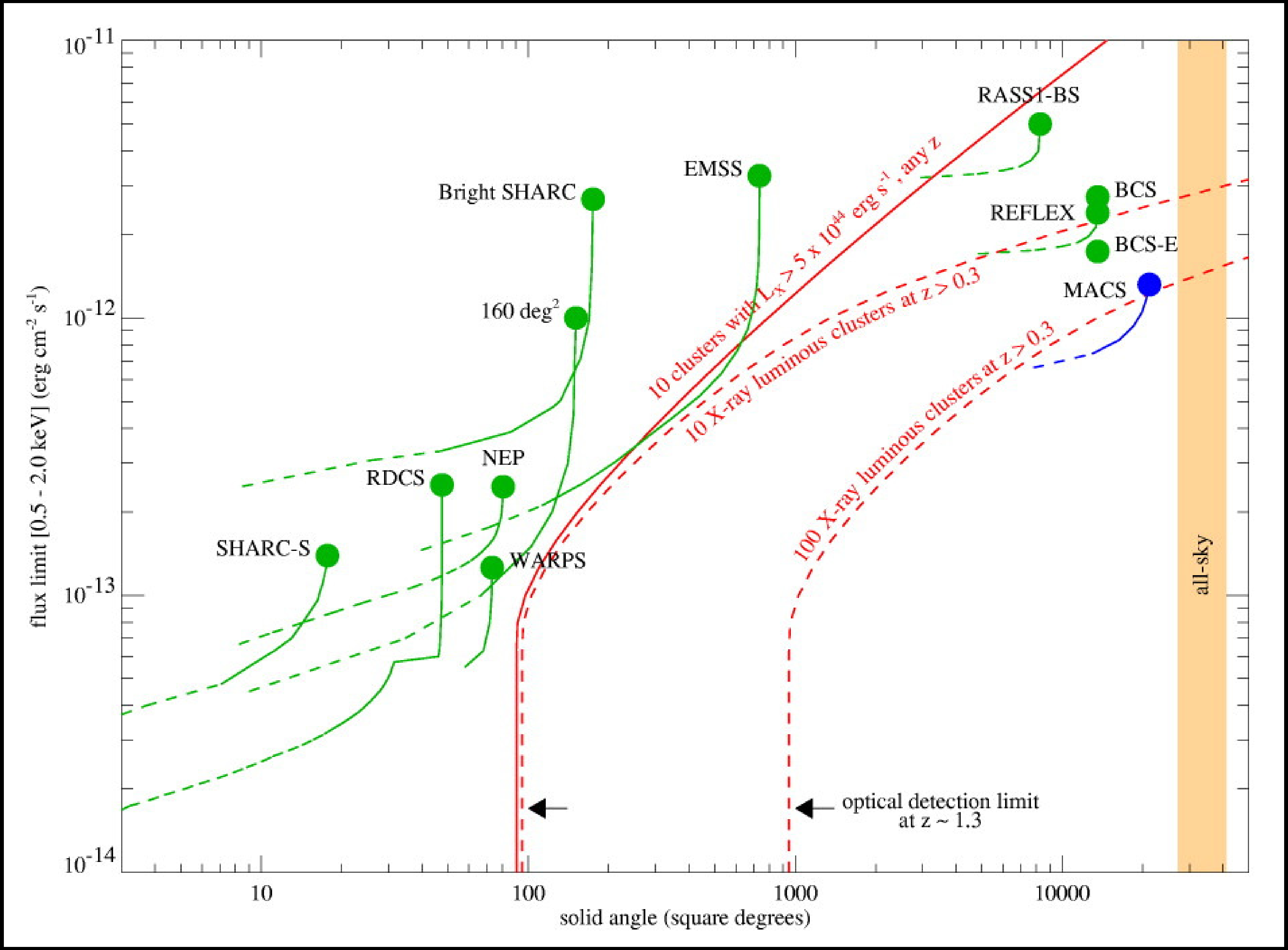

Ebeling et al. 2001

Galaxies in clusters

Observations of galaxies in clusters - Richness

- Richness is a measure of the total number of galaxies that belong to a cluster.
- "Rich" vs. "Poor" cluster
- It is very difficult to determine the total galaxy populations of a cluster because:
- 1) it depends on the mag. limit to which one counts
- 2) clusters don't have clear boundaries
- 3) There is contamination from foreground and background galaxies

Density Profiles

Density profiles provide information on the radial mass distribution, which can be related to theories of cluster formation.

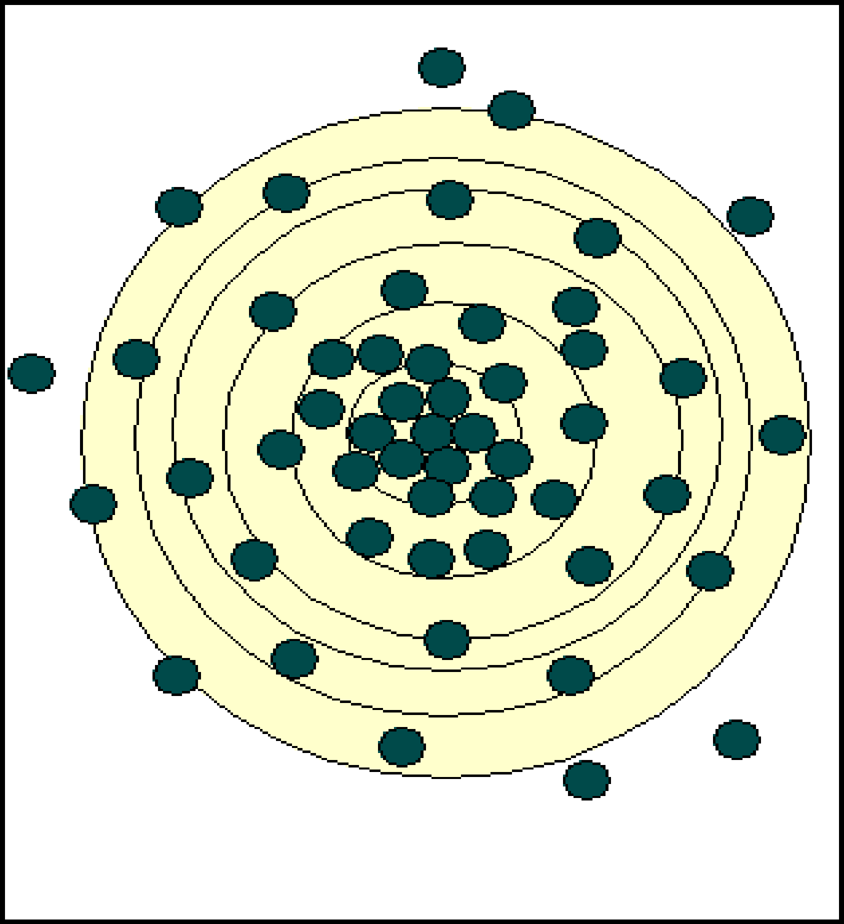

Density Profiles

Wiggles in the profile suggest substructure is present.

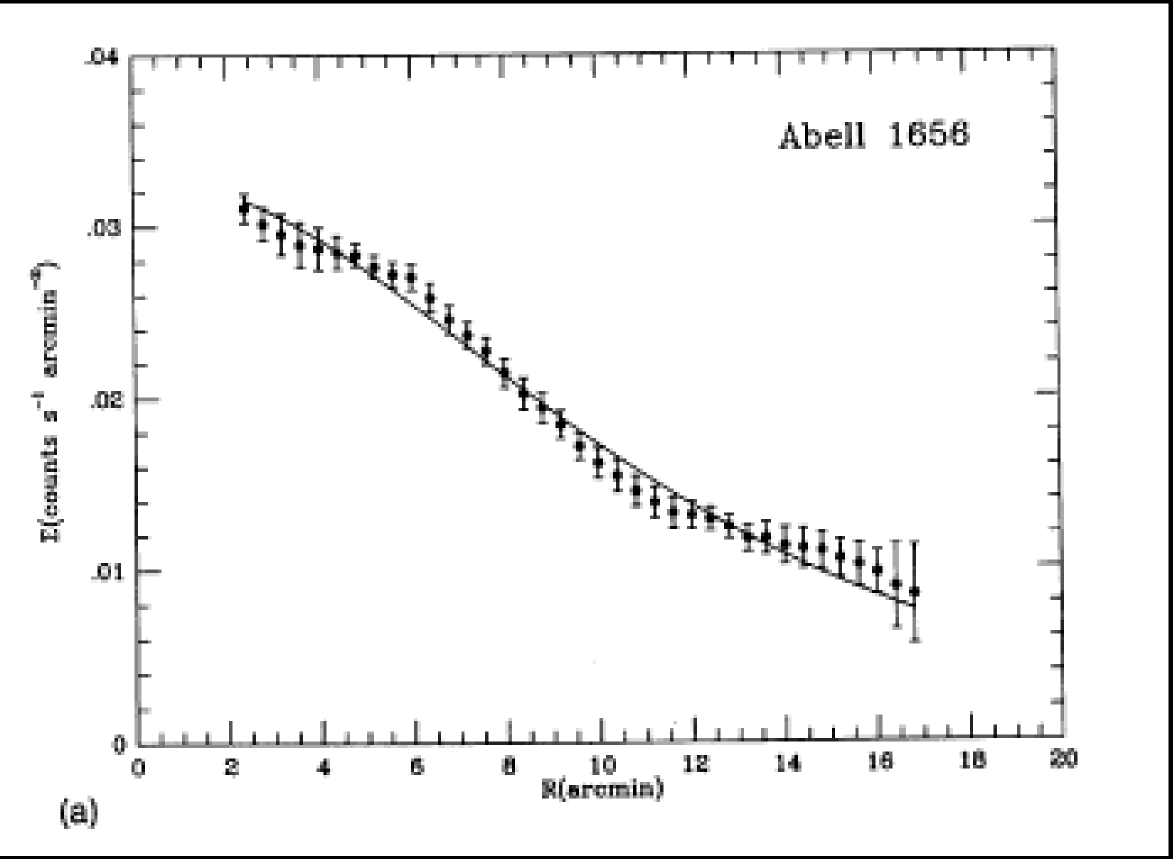

Density Profiles

Several different functional forms have been proposed to describe density profiles. Often more than one can fit the data.

- $\sigma(r) = \sigma_o\, r^{-\alpha}$ (power – law)
- $\sigma(r) = \sigma_o \exp\,[-7.67(r/r_e)^{1/4}]$ (de Vaucouleurs)
- $\sigma(r) = \sigma_o[1+(r/r_c)]^{-2}$ (Hubble profile)
- $\sigma(r) = \sigma_o[1+(r/r_c)^2]^{-1}$ (King profile)

Observations of galaxies in clusters – galaxy distribution

- Galaxy distributions in clusters show a wide range of morphologies, from smooth centrally-condensed to clumpy with no well-defined centroid.
- Many clusters are very elongated.

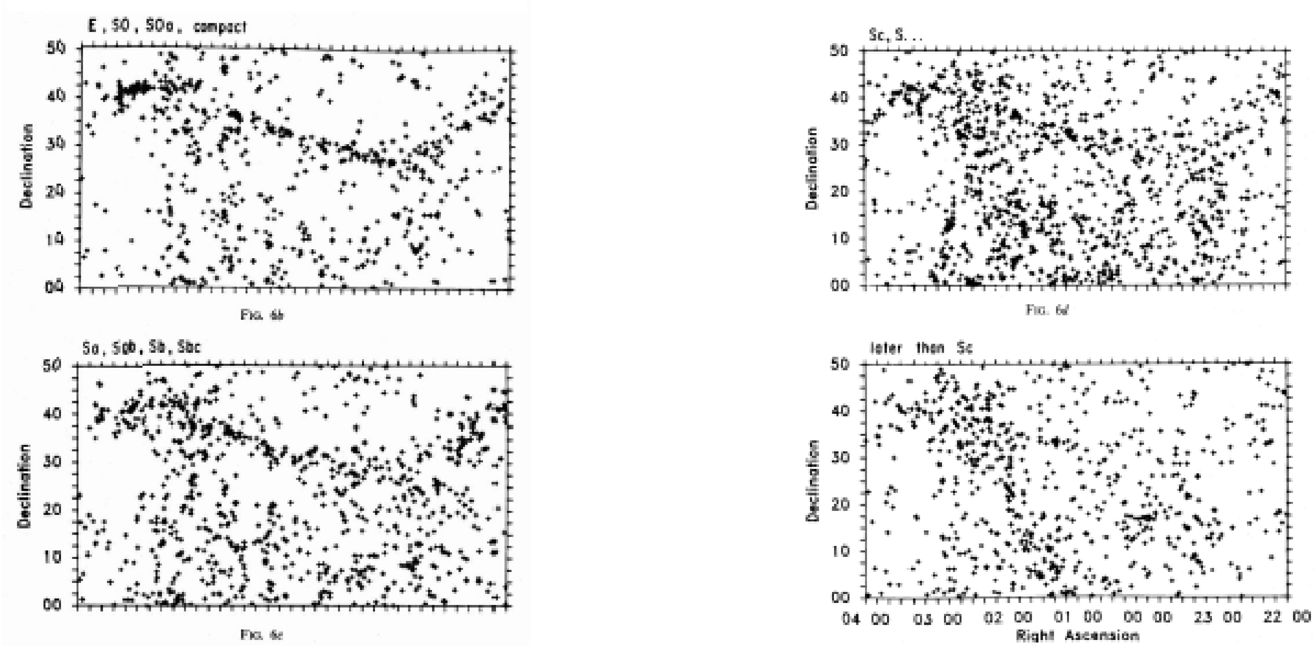

see: Giovanelli et al. (1986) *ApJ*, **300**, 77

Substructures

- Many clusters (about 50% or more) show substructure
- Dynamical evolution will rapidly erase substructure. Therefore its prevalence indicates that many clusters have formed fairly recently.
- If clusters are dynamically young, they may still carry clues about their initial conditions at the time of formation.

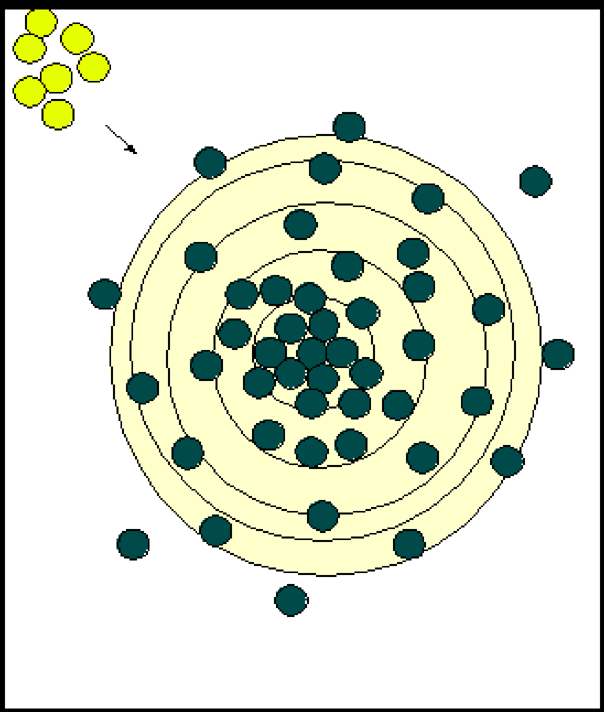

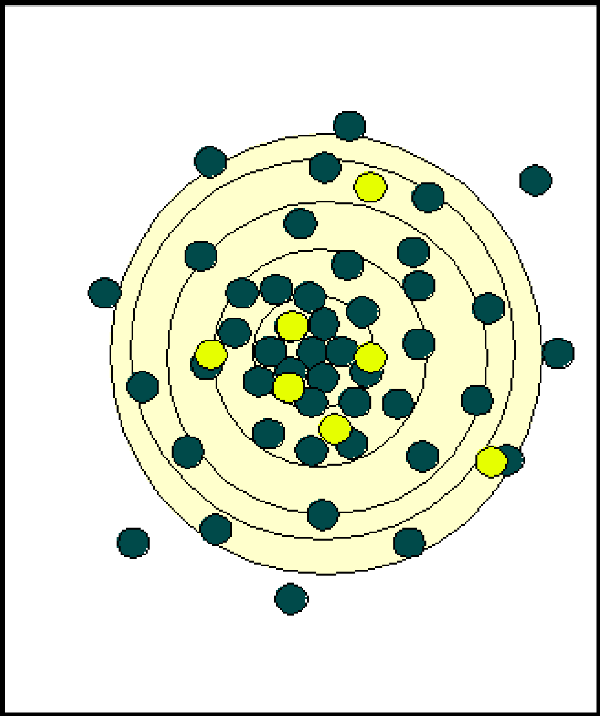

Observations of galaxies in clusters – galaxy populations

- The mixture of different galaxy types varies widely from cluster to cluster
- Poor clusters have a greater fraction of S and Irr. Rich clusters have a greater percentage of elliptical galaxies.

Morphology – density relation

- Galaxy type correlates with density; ellipticals are found preferentially in high-density regions

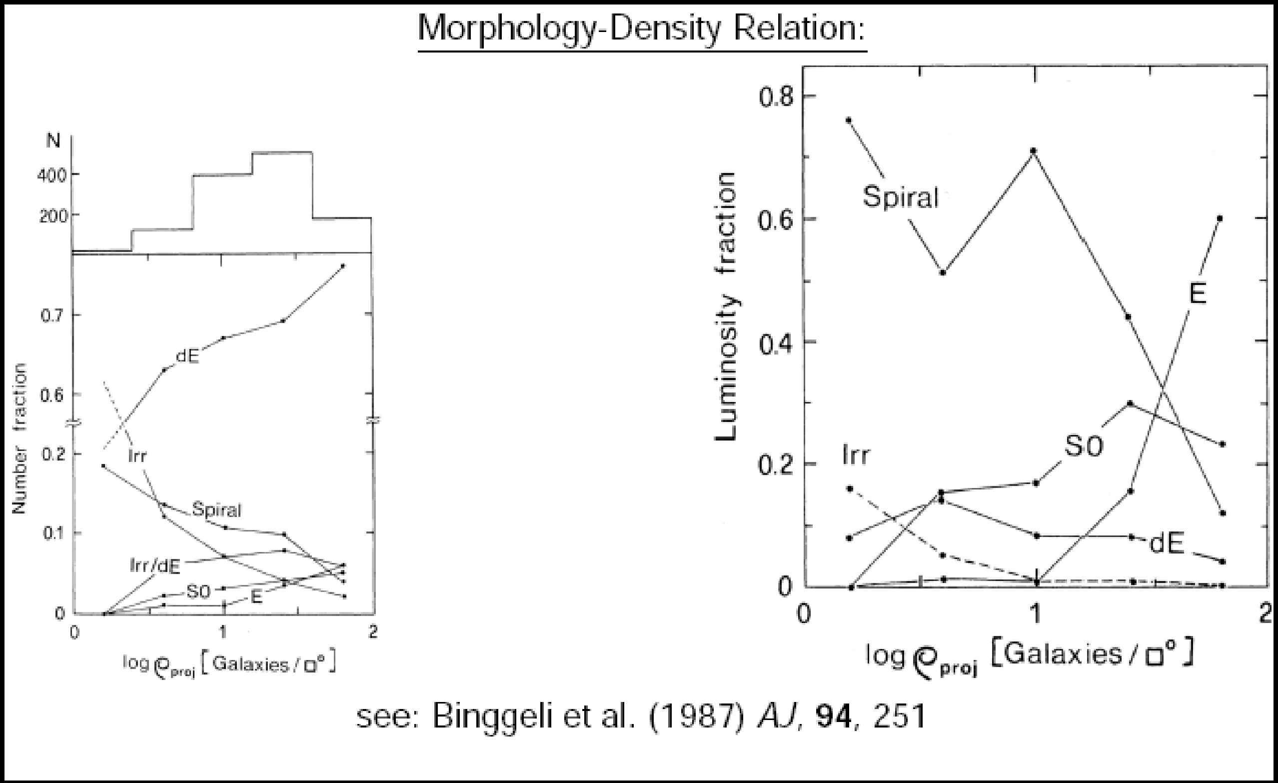

Morphology clustercentric-distance relation

- Galaxy type correlates with position; ellipticals are found preferentially near the cluster center.

Whitmore et al. 93

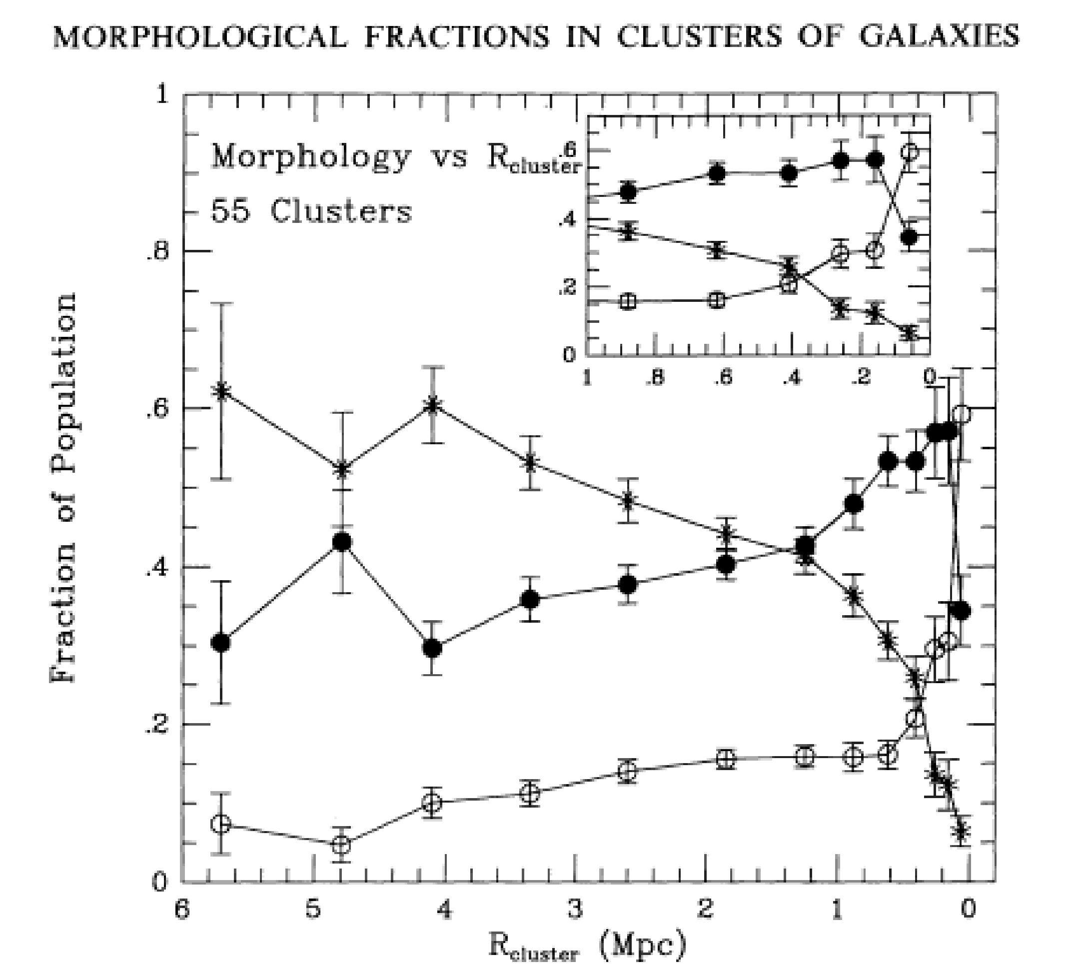

The colour-magnitude diagram

Clusters present the red-sequence, at low and intermediate redshifts

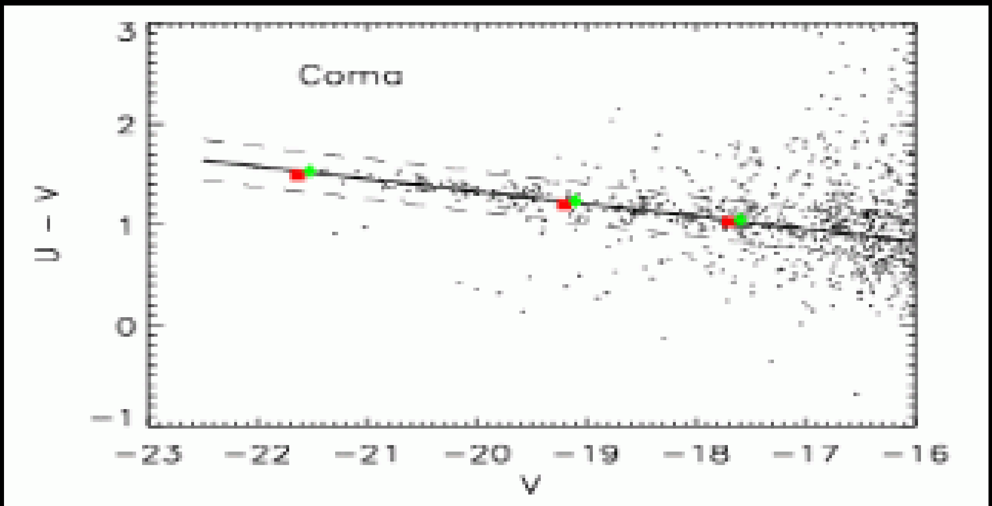

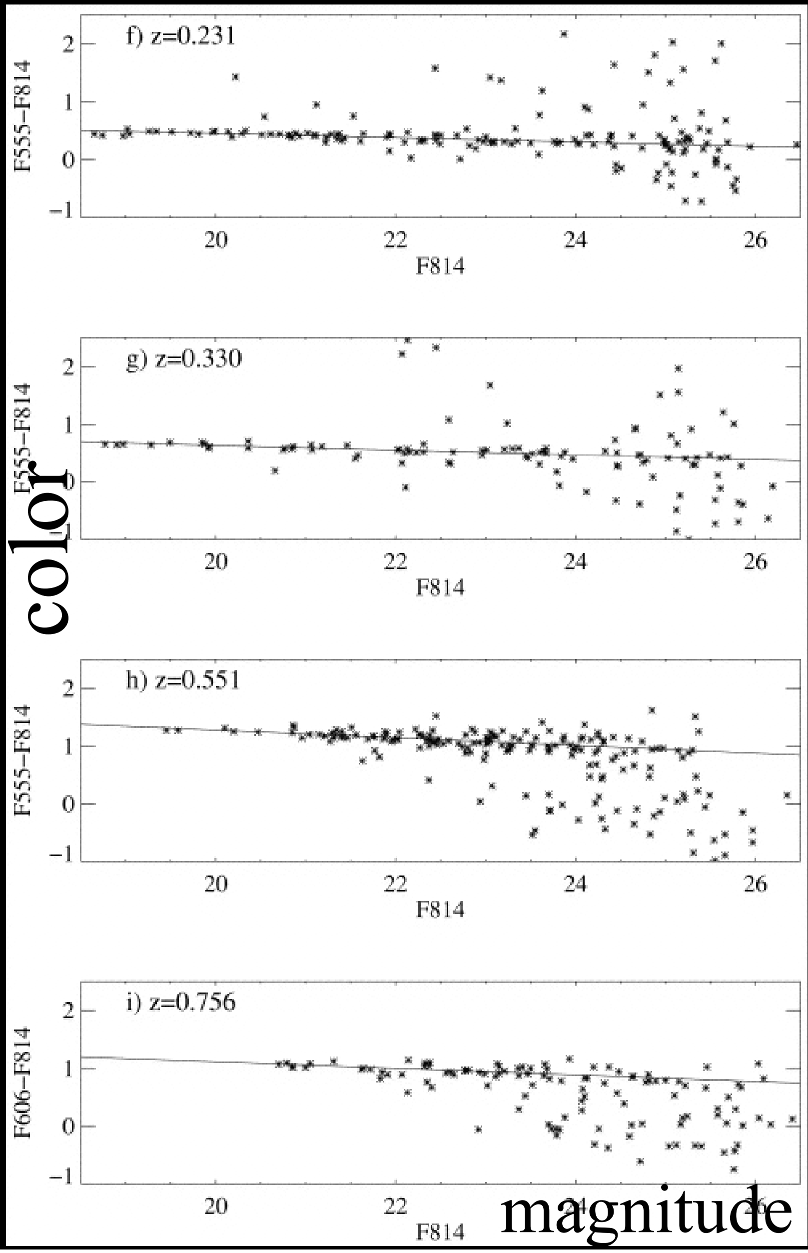

(Ellis et al; Kodama et al; Gladders et al)

Implications of the Color-magnitude relation of clusters

- Lopez-Cruz et al. (2004) studied the CMR for 57 X-ray detected Abell clusters
- “ Models that explain the CMR in terms of metallicity and passive evolution can naturally reproduce the observed behaviour of the CMRs studied”
- “The observed properties of the CMR are consistent with models in which the last episode of strong star formation in […] early-type galaxies in clusters were formed more than 7 Gyr ago”

The luminosity function of galaxies in clusters

Count number of galaxies in each bin of magnitudes

The luminosity function of galaxies in clusters

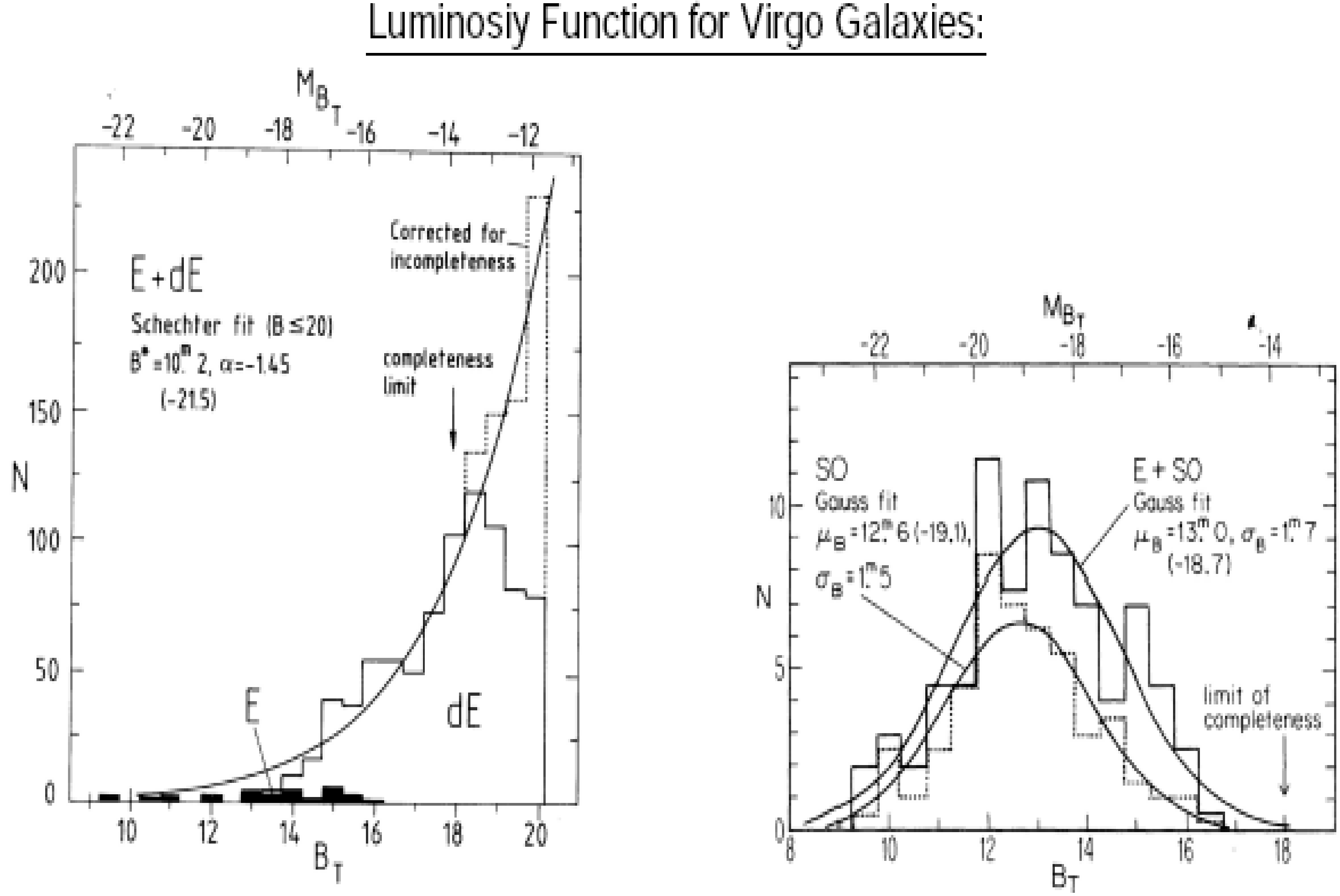

see: Sandage et al. (1985) *AJ*, **90**, 1759

The luminosity function of galaxies in clusters

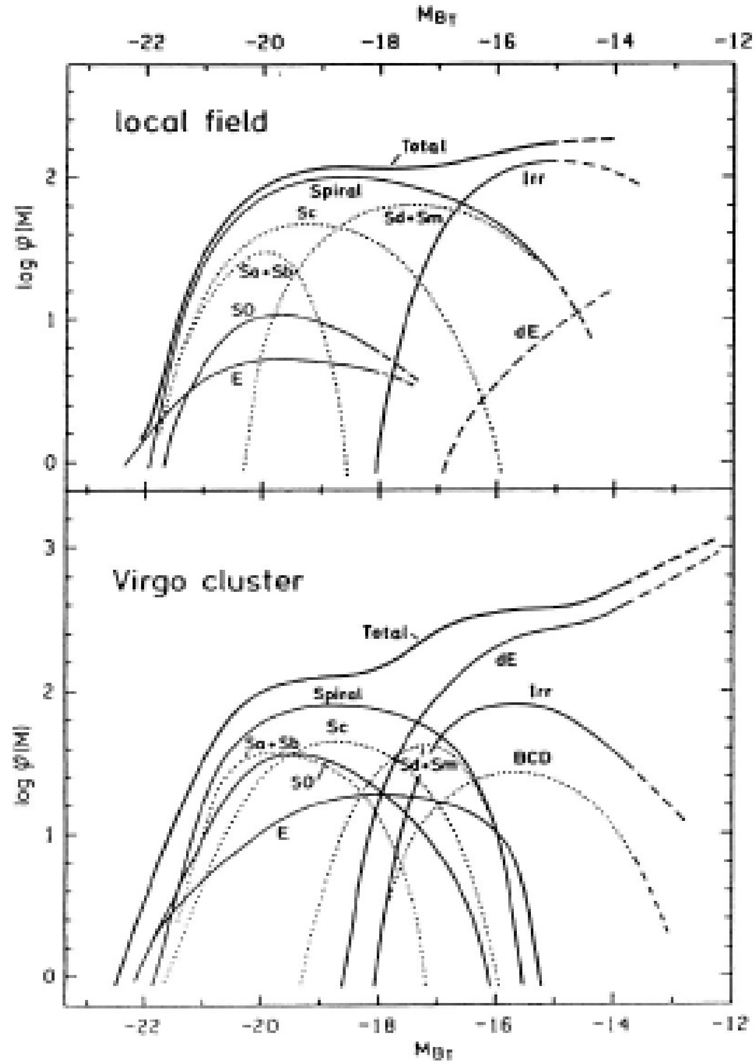

see: Sandage (1990) in *Clusters of Galaxies* Cambridge University Press

The luminosity function of galaxies in clusters

The luminosity function is usually well-described by a Schechter form:

$$\phi(L)dL = \phi^* \left(\frac{L}{L^*}\right)^{\alpha} exp\left(-\frac{L}{L^*}\right)\frac{dL}{L^*}$$

Where $\phi(L)$= the number of galaxies with luminosities L to L+dL

$L_* = 1 \times 10^{10} \quad h^{-2} L_\odot$

$\alpha = -1.0$ to -1.5

$\phi^* = 0.03\ h^3\ \mathrm{Mpc}^{-3}$

The luminosity function of galaxies in clusters

The Schechter function, in terms of magnitudes is:

$$\phi(M)dM = \frac{2}{5}\phi^*(ln10)\left[10^{\frac{2}{5}(M^*-M)}\right]^{\alpha+1} exp\left[-10^{\frac{2}{5}(M^*-M)}\right]dM$$

Luminosity function: What are M* and α ?

- The value of α indicates the dwarf content of the cluster
- For steep faint-end, $\alpha < -1$, the system is rich in dwarfs
- For a flat faint-end $\alpha = -1$
- For a declining faint-end $\alpha > -1$, few dwarfs
- M* is the knee of the function at the bright end

Coma Luminosity Function (Mobasher et al. 2003)

Over 700 galaxies with measured redshifts down to M_B= -16

They find a flat luminosity function with $\alpha \approx -1$

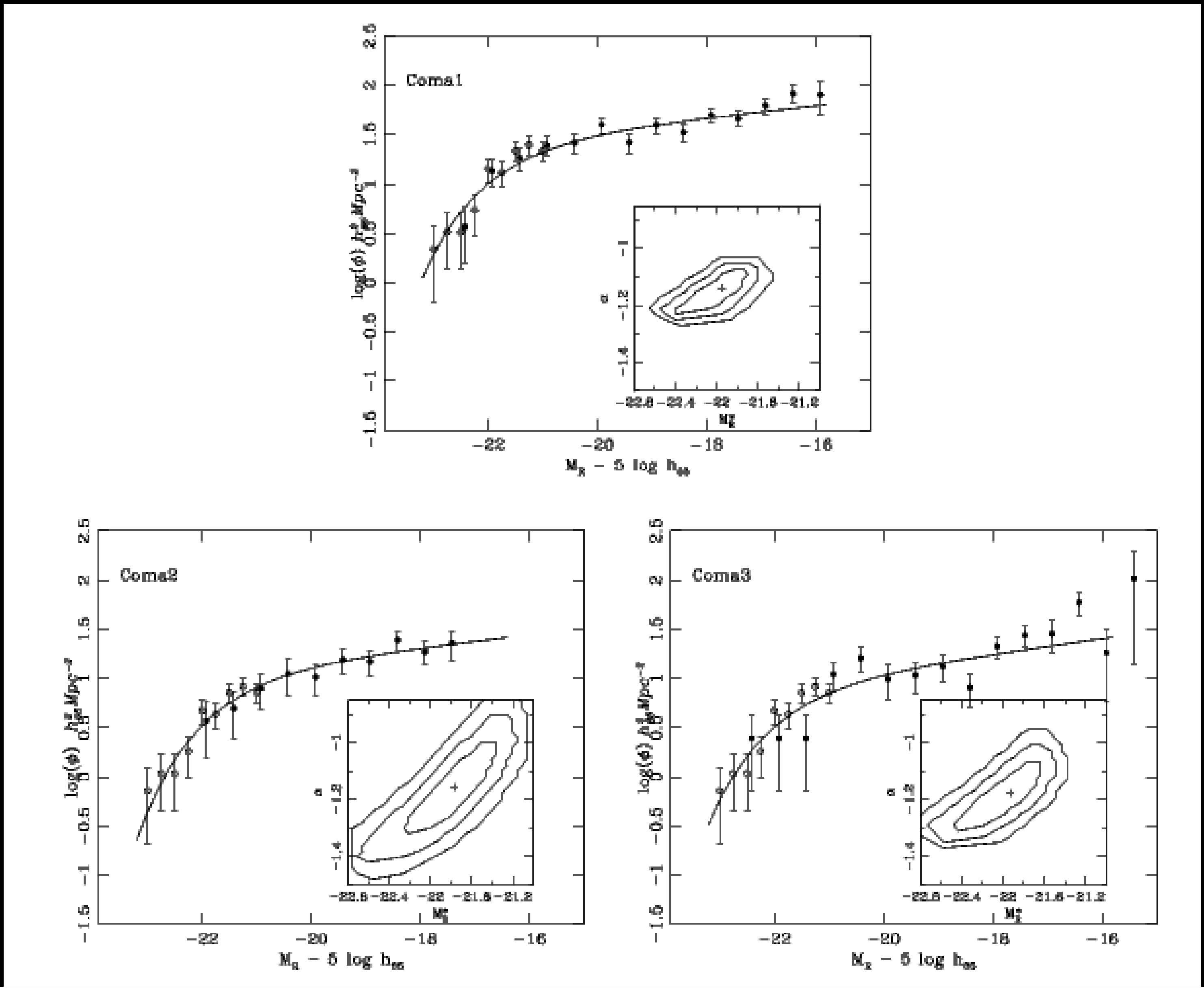

cD galaxies

cDs are the largest galaxies in the Universe, surrounded by faint envelopes which may extend for many hundreds of kpc.

They are found in the centers of clusters and of a few groups

They may have formed by galaxy canibalism or by accretion of tidally-stripped material from other galaxies

cD galaxies are often oriented in the same direction as the major axis of the cluster in which they reside

Originally studied to determine cosmological parameters (e.g. Sandage et al. 1972) and measure large-scale streaming motions (e.g. Lauer and Postman 1994).

cD galaxies

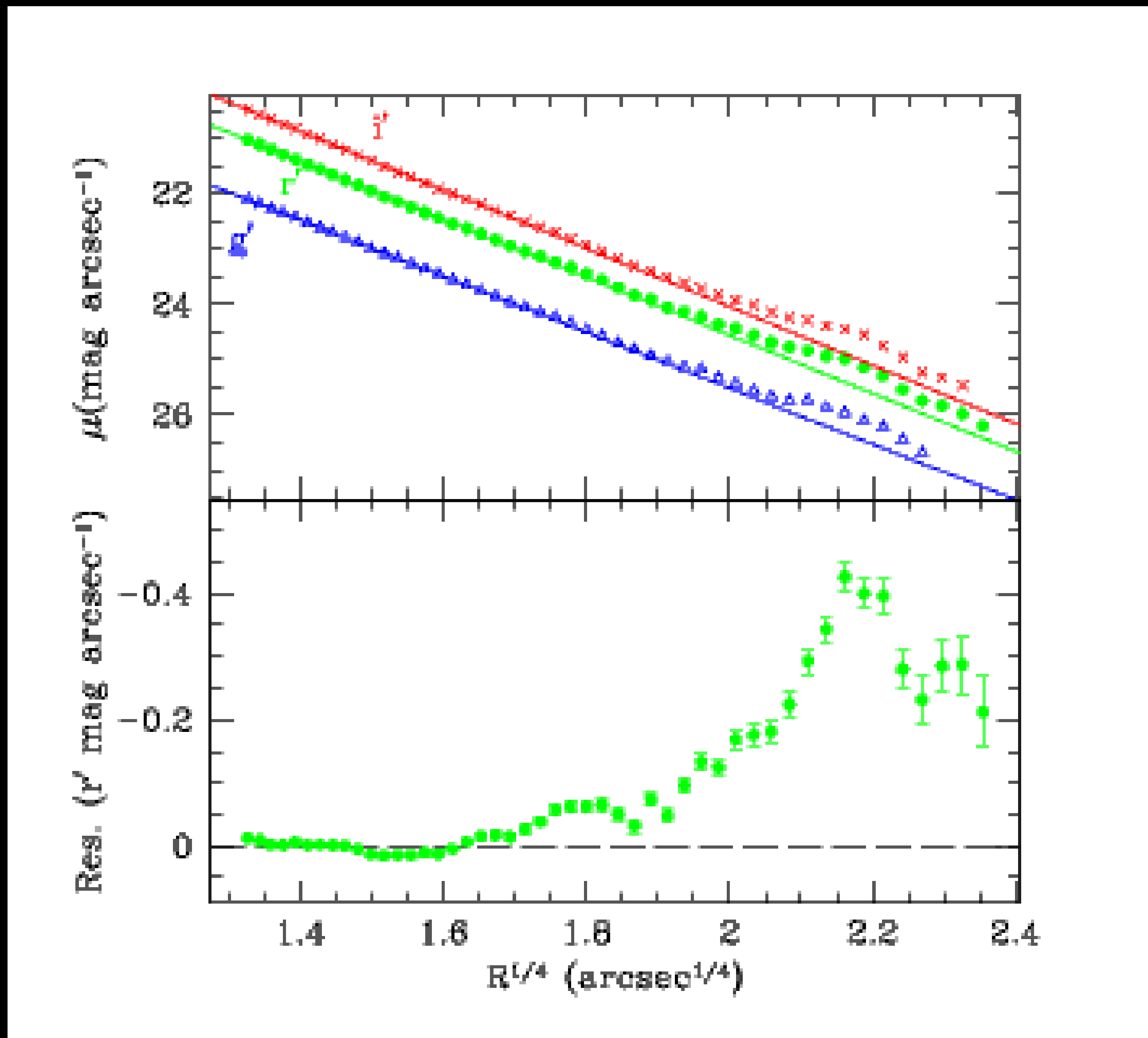

i'
r'
g'
22
24
26
−0.4
−0.2
0
1.4
1.6
1.8
2
2.2
2.4
R^{1/4} (arcsec^{1/4})
Res. (r' mag arcsec⁻¹)
μ(mag arcsec⁻¹)

Cluster kinematics – known long ago…

- In a cluster of galaxies the only important force acting between the galaxies is gravitation. It is the pulling of the galaxies on each other that gives rise to their velocities. The more mass in the cluster, the greater the forces acting on each galaxy (the higher the relative velocities).
- If the velocity of a given galaxy is too large, it will be able to escape the cluster. Therefore, by knowing that all of the galaxies have velocities of less than the escape velocity, one can estimate the total mass of a cluster.
- In the 30's, Zwicky and Smith examined the individual galaxies making up two nearby clusters (Coma and Virgo). What they found is that the velocities of the galaxies were about a factor of ten to one hundred larger than they expected.

Cluster kinematics

- Clusters are not static systems. Their galaxy populations are in contant motion.
- The speed of galaxies in clusters is characterised by the line-of-sight velocity dispersion

$$\sigma_{los} = \left[\frac{1}{N} \Sigma_{i=1}^{N} (v_i - < v >)^2 \right]^{1/2}$$

- If the galaxy orbits are isotropic, then:

$$\sigma_{3D} = (\sigma_x^2 + \sigma_y^2 + \sigma_z^2)^{1/2} = 3^{1/2} \sigma_{los}$$

Cluster kinematics

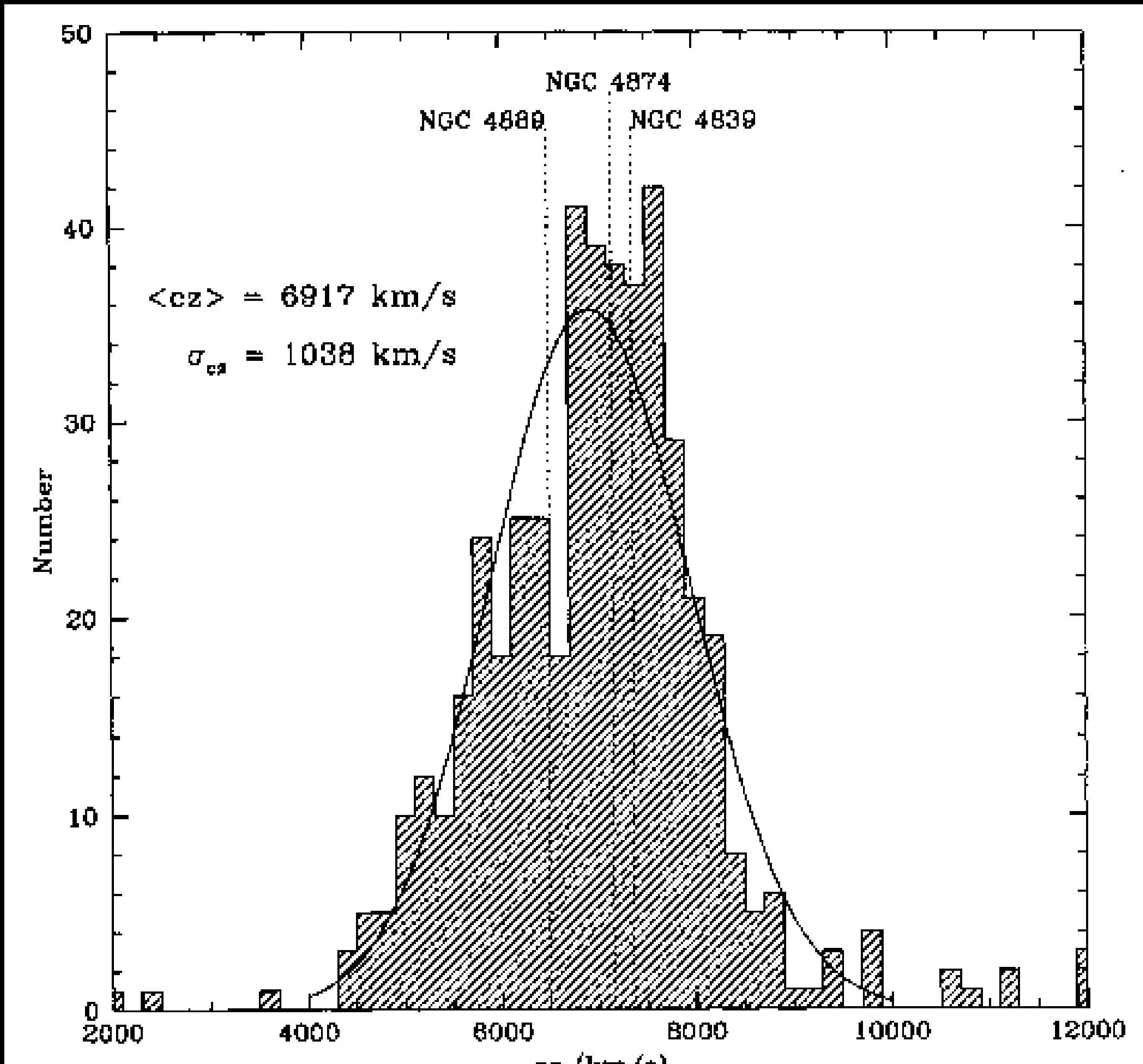

Velocity Distribution In the Coma Cluster (552 velocities)

Coless and Dunn (1996)

Cluster kinematics

- The shape of the velocity distribution gives information about the dynamical state of the cluster.
- Significant deviations from Gaussian may indicate non-isotropic orbits or subclustering.
- These can be measured from moments of the velocity distribution.
- 1st moment = <v>
- 2nd moment = σ
- 3rd moment =
- 4th moment =

$$Skewness = \frac{1}{N}\Sigma_{i=1}^{N}\left[\frac{v_i - < v >}{\sigma}\right]^3$$

$$Kurtosis = \frac{1}{N}\Sigma_{i=1}^{N}\left[\frac{v_i - < v >}{\sigma}\right]^4 - 3$$

How to weigh a cluster of galaxies: the Virial Theorem

- A self-gravitating system in a steady-state will satisfy the virial theorem: 2T+U=0, where T=kinetic energy and U=potential energy. Hence,

$$\frac{1}{2}M_{cl}\sigma^2 - \frac{\alpha G M_{cl}^2}{R} = 0$$

where α depends on the matter distribution

$\alpha = 3/5$ for a uniform sphere

$\alpha \sim 1$ for typical profiles

This yields,

$$M_{cl} \sim 10^{15} M\odot \left(\frac{\sigma_{los}}{10^3 km/s}\right)^2 \left(\frac{R}{1Mpc}\right)$$

– Virial estimates indicate total cluster masses $M_{cl} \sim 10^{13}$–10^{15} $M\odot$

– Visible galaxies account for only $\sim 5-10\%$ of M_{cl}

Physical processes affecting cluster galaxies

- Ram pressure stripping (Gunn and Gott 1972, Quilis et al. 2000)
- Tidal effects, mergers and accretion (Toomre and Toomre 1972, Bekki 2001, Aguerri et al. 2001)
- Harassment (Moore et al. 1996, Mastropietro et al. 2004) – Transformation of a late-type spiral galaxy into a dwarf galaxy through interactions between cluster galaxies and with the gravitational cluster potential

Interaction of a galaxy with the cluster environment

Gravitational interaction galaxy - cluster

Gravitational interaction galaxy - galaxy

Ram pressure: galaxy ISM – intracluster medium (ICM)

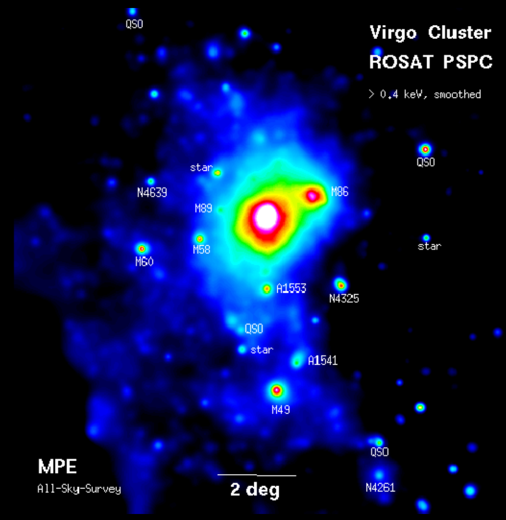

(Böhringer et al. 1994)

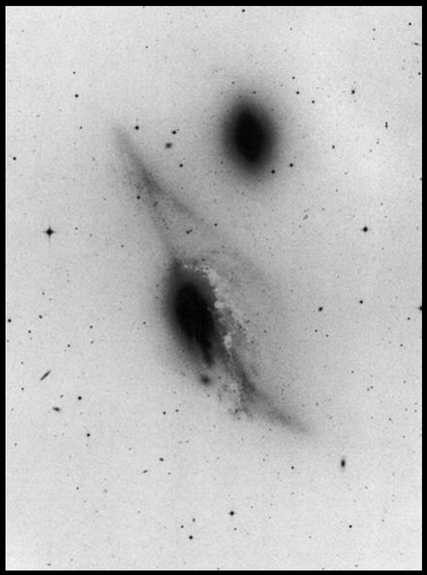

(Kenney et al. 1995)

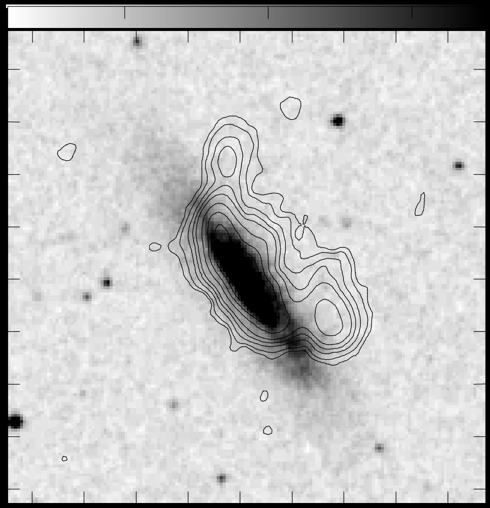

Spiral galaxies in the Virgo cluster

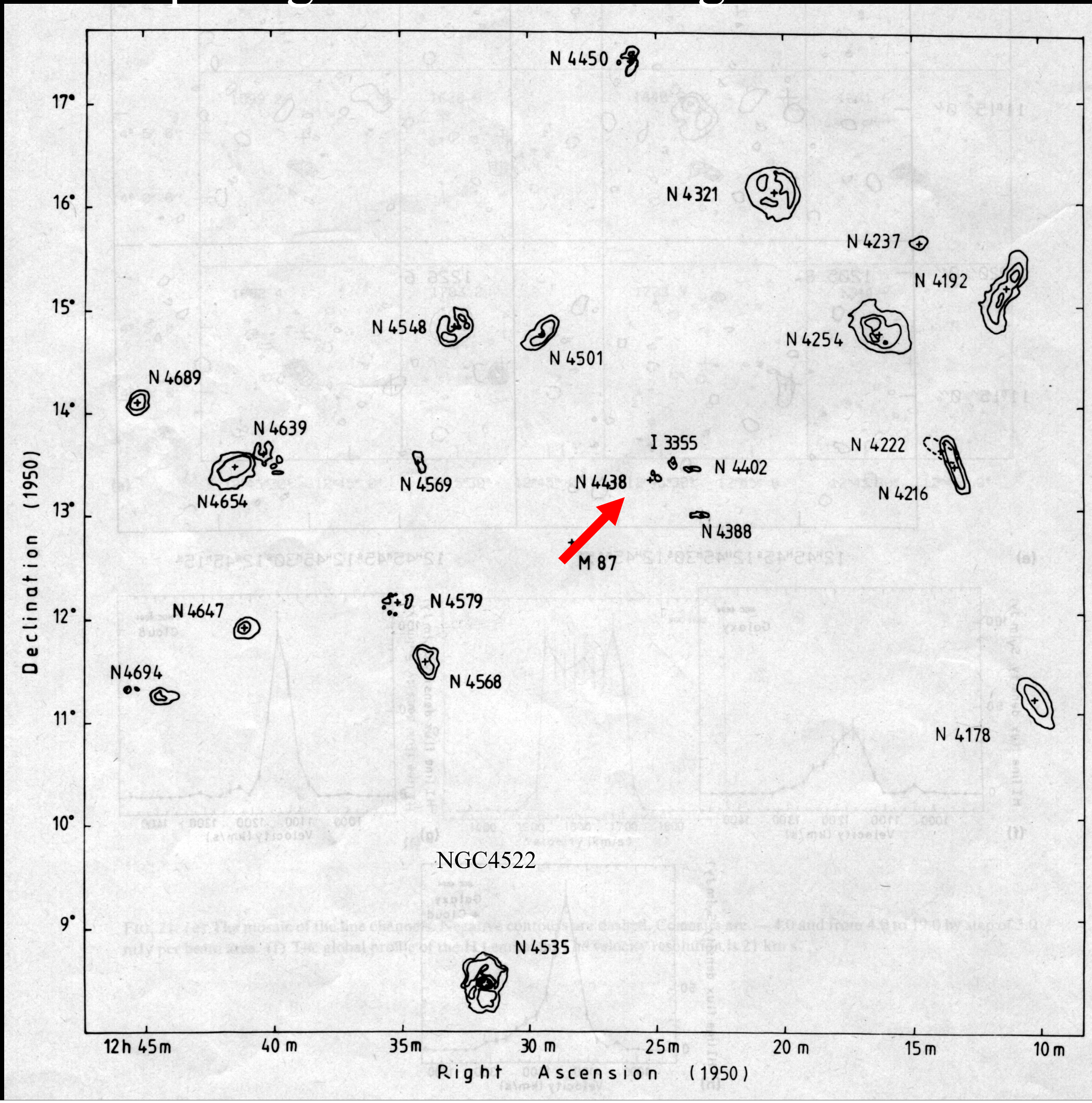

NGC 4438

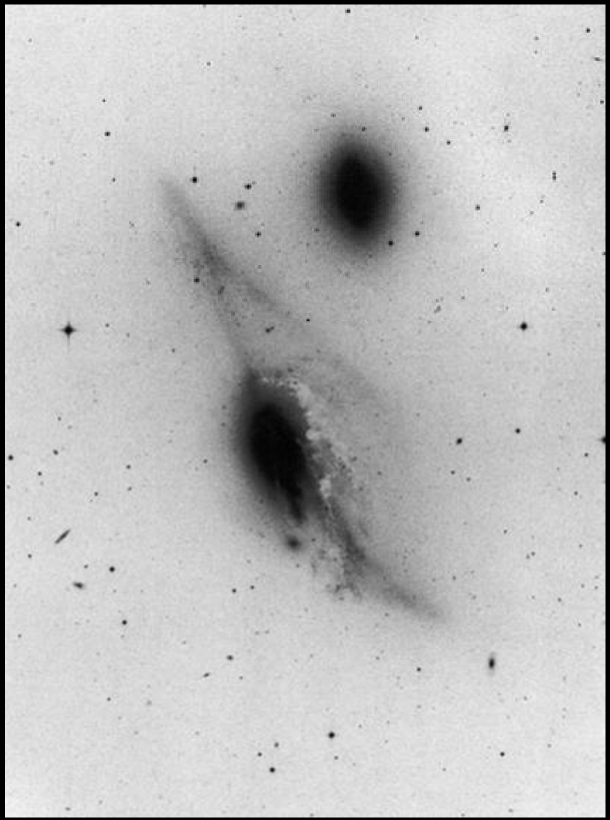

(Kenney et al. 1995)

Color: optical B band
Spectra: IRAM 30m CO(1-0)

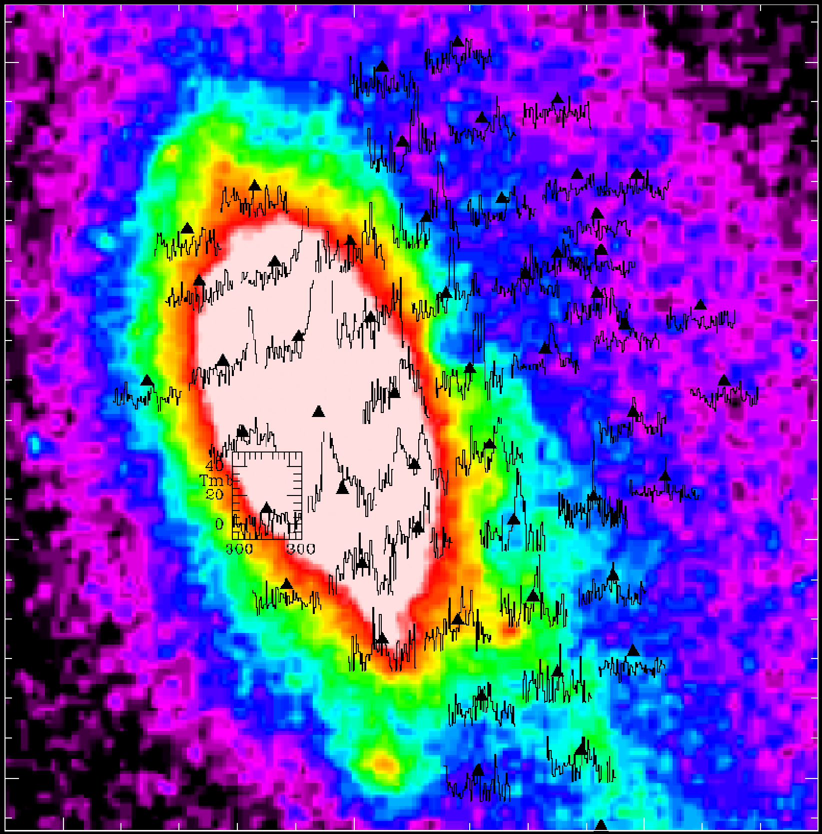

(Vollmer et al. 2004)

NGC 4438

Grey: gas   Contours: stars

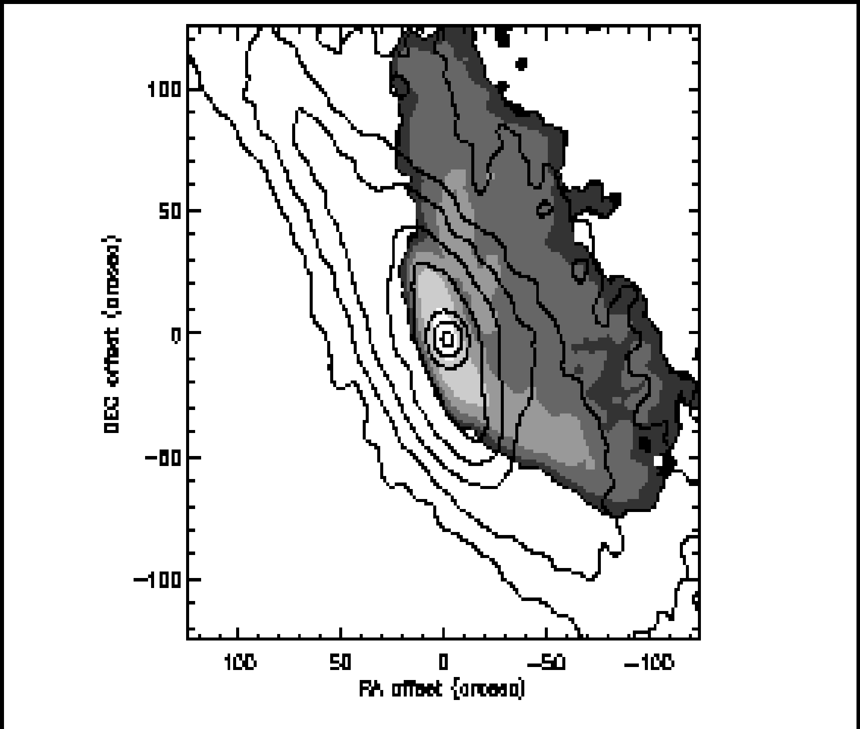

Summary to remember!

- Clusters of galaxies are a very diverse class of objects
- Many (50% or more) of clusters show significant substructure in their galaxy distributions.
- Member galaxies span an enormous range of luminosities and morphological mixtures. Elliptical galaxies prefer dense environments.
- The distribution of galaxy velocities can provide information on the dynamical state of a cluster.
- Cluster masses can be measured from the virial theorem.
- Cluster masses range from 10^{13}-10^{15} $M_{\odot}$. Galaxies account for only 5-10% of this mass, and hence most of the cluster mass must be dark.

The intracluster medium

Clusters are among the most luminous X-ray sources in the sky. This X-ray emission comes from hot intracluster gas.

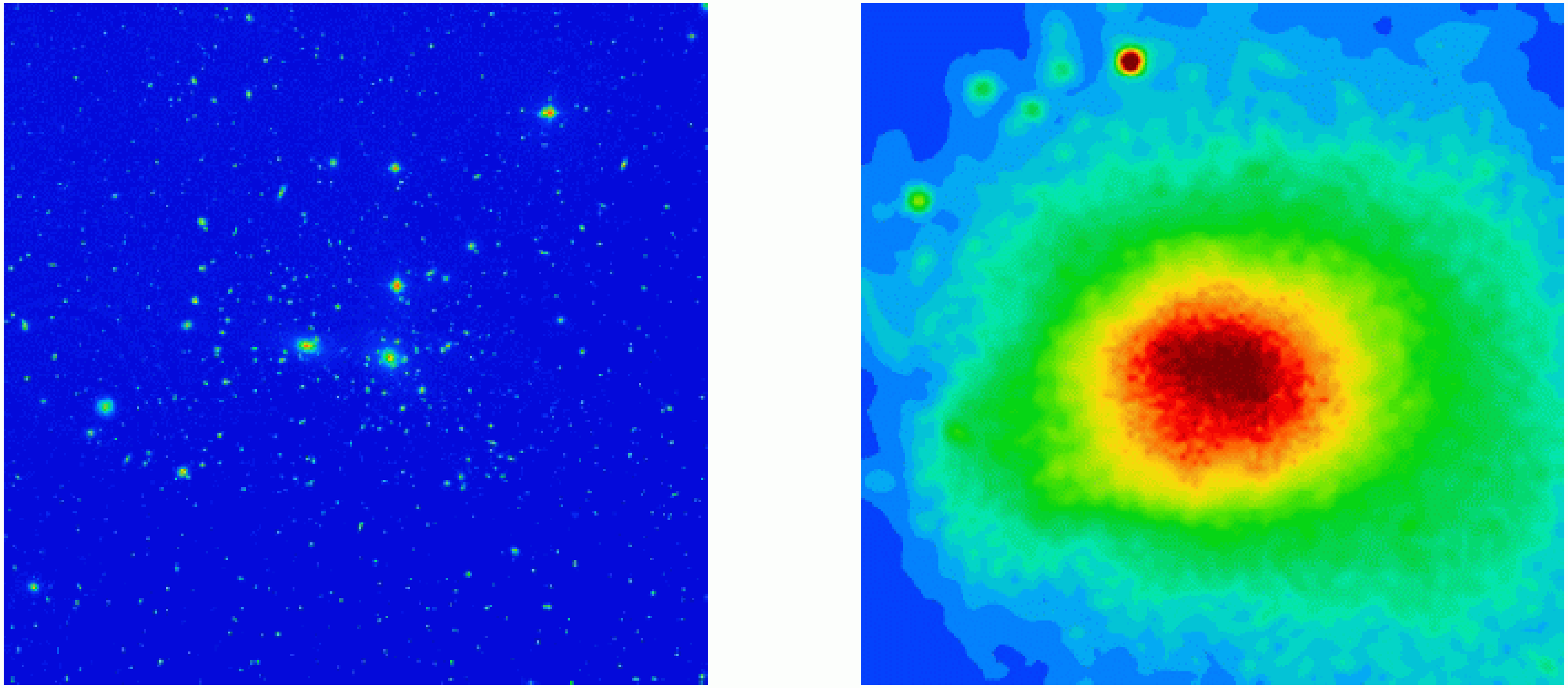

Coma cluster

X-ray observations provide information on the amount, distribution, temperature and chemical composition of the intracluster gas

For comparison,

- Cataclismic variables $L_x = 10^{32} – 10^{38}$ erg/s
- Milky Way, M31 $L_x = 10^{39}$ erg/s
- Clusters of galaxies $L_x = 10^{43} – 10^{45}$ erg/s
- Only Seyferts, QSOs, and other AGN rival clusters in X-ray output
- Clusters may emit nearly as much energy at X-ray wavelengths as visible

$$L(\text{optical}) = 100\ L^*\ \text{galaxies} = 10^{45}\ \text{erg/s}$$

The L_x – σ correlation

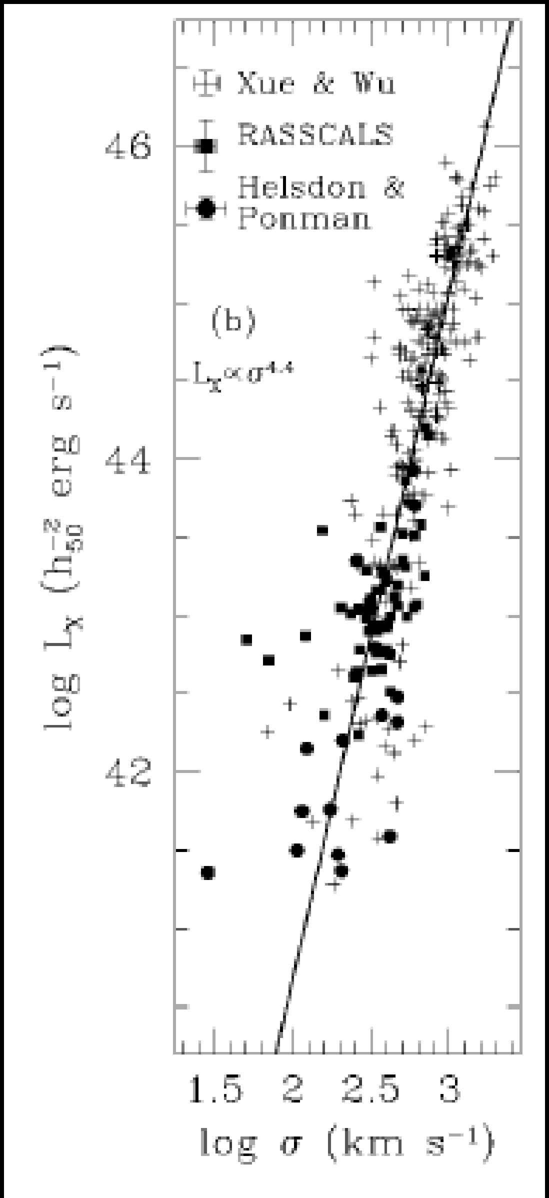

Origin of cluster X-ray emission

- Hot (10^7 – 10^8 K) low-density (10^{-3} cm^{-3}) gas, mostly H and He, between galaxies. At these high temperatures the gas is fully ionized.
- Two emission mechanisms:

  1) Thermal bremsstrahlung (important for T > 4 x 10^7 K)

  free electrons may be rapidly accelerated by the attractive force of atomic nuclei, resulting in photon emission

  because the emission is due to Coulomb collisions, X-ray luminosity is a function of gas density and temperature

$$Lx = n_{electron}\, n_{ion}\, T^{1/2} = \rho_{gas}^{\ 2}\ T_{gas}^{\ 1/2}$$

2) Recombination of electrons with ions (important T < 4 x 10^7 K)

Dynamics of the intracluster gas

The intracluster gas can be treated as:

- An ideal fluid
- In hydrostatic equilibrium
- At a uniform temperature

Why a fluid?

– The mean-free path for an electron to collide with an ion is

$$\lambda_e = \frac{distance - travelled}{number - of - collisions} \sim \frac{v_e t}{n\sigma v_e t} \sim \frac{1}{n\sigma}$$

where v_e = electron speed; n=number density of ions; t=time interval

and σ = collisional cross-section.

– Strong collisions will occur when kinetic energy of the electron

is comparable to potential energy at closest approach, b,

$$\frac{1}{2}m_e v_e^2 \sim \frac{qe}{4\pi\epsilon_0 b} = 0$$

where

q= charge of ion; e= charge of electron; ϵ_0 = permissivity of space.

– The cross-section for strong collisions is thus

$$\sigma = \pi b^2 \sim \frac{q^2 e^2}{4\pi \epsilon_0^2 m_e^2 v_e^4} = 0 \tag{5}$$

– A more realistic treatment, which includes the effects of both nearby and distant collisions increases σ by a factor $\sim \ln\Lambda$, where $\ln\Lambda$ = the Coulomb logarithm (ratio of largest to smallest collision impact parameters b_{max}/b_{min}

– Once the gas has reached thermal equilibrium

$$m_e v_e^2 \sim m_{ion} v_{ion}^2 \sim 3 k_b T \tag{6}$$

k_B = Boltzmann constant and T= gas temperature

– Hence

$$\lambda_e \sim \lambda_i \sim 20kpc \left(\frac{T}{10^8 K}\right)\left(\frac{n}{10^{-3} cm_{-3}}\right)^{-1} \tag{7}$$

– Since $\lambda_e << $ size of cluster, the intracluster gas can be treated as a collisional fluid.

Why hydrostatic equilibrium?

– The intracluster gas will respond to changes at a rate determined by the sound speed.

– The sound speed in an ideal monatomic gas is

$$v_{sound} \sim \sqrt{\frac{5k_BT}{3\mu m_H}} \tag{11}$$

where μ = mean molecular weight of gas and m_H = mass of proton

– The time for a sound wave to cross a cluster of diameter d is

$$t_{sound} \sim \frac{d}{v_{sound}} \sim 7 \times 10^8 \left(\frac{T}{10^8 K}\right)^{-1/2} \left(\frac{d}{1 Mpc}\right)^{-1} years \tag{12}$$

– Because $t_{sound} << t_{cool}$ the gas will be in hydrostatic equilibrium (gas pressure balances gravity). For a spherical mass distribution,

$$\frac{1}{\rho_{gas}}\frac{dP}{dr} = -\frac{d\Phi}{dr} = -\frac{GM(r)}{r^2} \tag{13}$$

Because the gas is in hydrostatic equilibrium in the cluster potential well, its distribution maps the cluster's mass distribution.

Why a single temperature?

– Frequent collisions between electrons and ions exchange energy. This leads to a Maxwellian distribution of particle velocities. Velocities are isotropic.

– The timescale for redistribution of energy between electrons is

$$t_{eq}(e,e) \sim \frac{\lambda_e}{v_e} \sim 3\times10^5 \left(\frac{T}{10^8 K}\right)^{3/2} \left(\frac{n}{10^{-3}cm^{-3}}\right)^{-1} years \tag{8}$$

– Similarly, the timescale for electrons and ions to reach thermal equilibrium is

$$t_{eq}(e,i) \sim \left(\frac{m_p}{m_e}\right) t_{eq}(e,e) \sim 6\times10^8 \left(\frac{T}{10^8 K}\right)^{3/2} \left(\frac{n}{10^{-3}cm^{-3}}\right)^{-1} years \tag{9}$$

– X-ray emission by thermal bremsstrahlung cools the gas on a timescale

$$t_{cool} \sim 8\times10^{10} \left(\frac{T}{10^8 K}\right)^{1/2} \left(\frac{n}{10^{-3}cm^{-3}}\right)^{-1} years \tag{10}$$

– Since $t_{eq} << t_{cool}$, the intraclutser gas can be characterized by a single temperature T_{gas} for both electrons and ions.

Why a single temperature?

– Frequent collisions between electrons and ions exchange energy. This leads to a Maxwellian distribution of particle velocities. Velocities are isotropic.

– The timescale for redistribution of energy between electrons is

$$t_{eq}(e,e) \sim \frac{\lambda_e}{v_e} \sim 3 \times 10^5 \left(\frac{T}{10^8 K}\right)^{3/2} \left(\frac{n}{10^{-3} cm^{-3}}\right)^{-1} years \tag{8}$$

– Similarly, the timescale for electrons and ions to reach thermal equilibrium is

$$t_{eq}(e,i) \sim \left(\frac{m_p}{m_e}\right) t_{eq}(e,e) \sim 6 \times 10^8 \left(\frac{T}{10^8 K}\right)^{3/2} \left(\frac{n}{10^{-3} cm^{-3}}\right)^{-1} years \tag{9}$$

– X-ray emission by thermal bremsstrahlung cools the gas on a timescale

$$t_{cool} \sim 8 \times 10^{10} \left(\frac{T}{10^8 K}\right)^{1/2} \left(\frac{n}{10^{-3} cm^{-3}}\right)^{-1} years \tag{10}$$

– Since $t_{eq} << t_{cool}$, the intraclutser gas can be characterized by a single temperature T_{gas} for both electrons and ions.

X-ray spectra

- Spectroscopy of the intracluster gas provides information on its temperature and composition
- Observed spectra show exponential decrease at high-frequencies that is characteristic of bremsstrahlung.

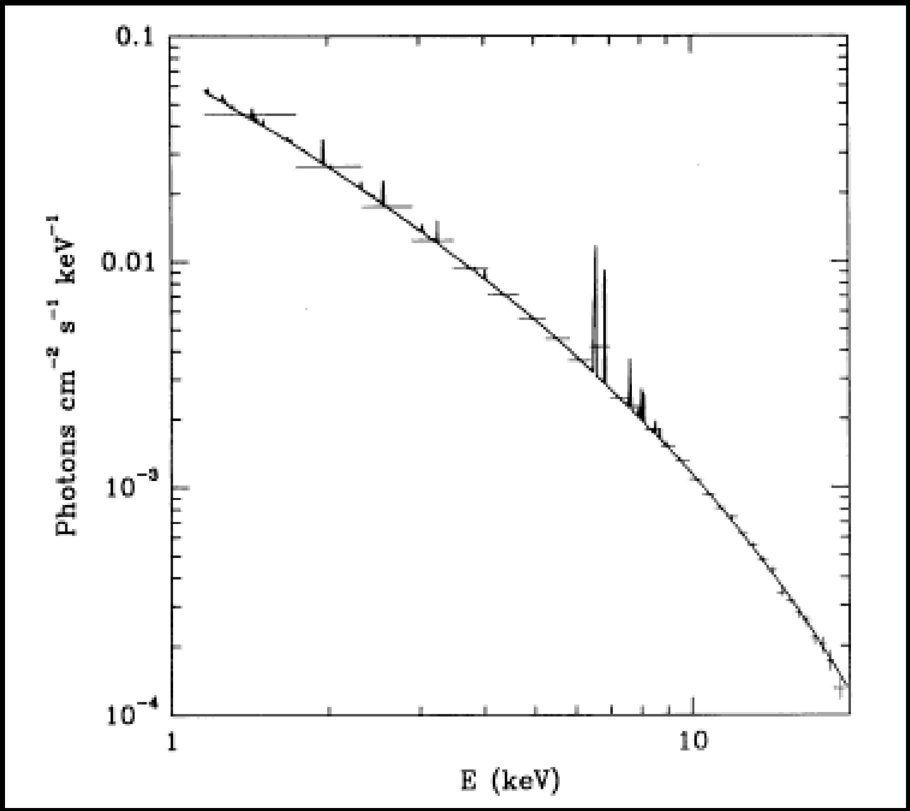

Coma Cluster
(Hughes et al. 93)

- Emission lines due to Fe, Ni and other heavy elements are seen. This suggests that much of the intracluster gas must have been processed through stars.
- Chemical abundance of the intracluster gas can be measured from the equivalent widths of these emission lines. It is found to be about $0.3\text{-}0.4Z_{\odot}$
- If the galaxies and gas are both in thermal equilibrium in the cluster potential well, then one expects

$$m_{\mathrm{gal}}\, v_{\mathrm{gal}}^{2} = 3\, k_{\mathrm{b}} T_{\mathrm{gas}}$$

Origin of the intracluster gas

Two possibilities:

- The intracluster gas once resided in galaxies and was later removed.

  - this would explain high metallicity of gas

  - galaxies in the cores of rich clusters are observed to be deficient in HI gas, which suggests that stripping has occurred.

  - but since $M_{gas} >> M_{gal}$ it is difficult to understand how so much material could have been stripped from galaxies

- The gas is primordial, originating at the time of cluster formation.

  - but $0.3\text{-}0.4Z_{\odot}$

How much gas is there in clusters?

The observed X-ray surface brightness profiles have a radial distribution

$$\Sigma_X(r) = \Sigma_0 \left[1 + \left(\frac{r}{r_C}\right)^2\right]^{-3/2} \quad (1)$$

Assuming spherical symmetry, constant temperature and X-ray emission proportional to $\rho(\text{gas})^2$, then this corresponds to a spatial gas density of

$$\rho_{gas}(r) = \rho_0 \left[1 + \left(\frac{r}{r_C}\right)^2\right]^{-1} \quad (2)$$

$$\rho_{gas}(r) \propto r^{-2}, \text{ at large r} \quad (3)$$

This can be integrated to determine the total gas mass M_{gas} within distance R of the cluster center

$$M_{gas}(< R) = \int_0^R \rho_{gas}(r) 4\pi r^2 dr \quad (4)$$

Observations indicate that the total gas mass in clusters is usually several times greater than the total galaxy mass

Cluster Mass estimates: X-ray gas

Assuming that the intracluster gas is in hydrostatic equilibrium in the cluster potential well, the **total** cluster mass can be found:

$$\frac{1}{\rho_{gas}}\frac{dP}{dr} = \frac{d\phi}{dr} = -\frac{GM_{cl}(r)}{r^2} \tag{5}$$

Substituting the ideal gas law, P=$\rho k_b T/\mu m_H$ and solving for M(R)

$$M_{cl}(< R) = -\frac{k_b T_{gas}}{\mu m_H G}\left(\frac{\delta ln \rho_{gas}}{\delta ln r} + \frac{\delta ln T_{gas}}{\delta ln r}\right) \tag{6}$$

Note that M_{cl} depends sensitively on T_{gas} but weakly on ρ_{gas}. In principle, radial gradients in ρ_{gas} and T_{gas} are observable. In reality, temperature gradients are very difficult to detect.

A simplifying assumption is that the gas is **isothermal**, then

$$\frac{\delta ln T_{gas}}{\delta ln r} = 0 \tag{7}$$

$$M(< R) = -\frac{k_b T_{gas}}{\mu m_H G}\left(\frac{\delta ln \rho_{gas}}{\delta ln r}\right) \tag{8}$$

The total gas mass in clusters exceeds the total galaxy mass. Gas contributes as much as 10-20% of the total cluster mass.

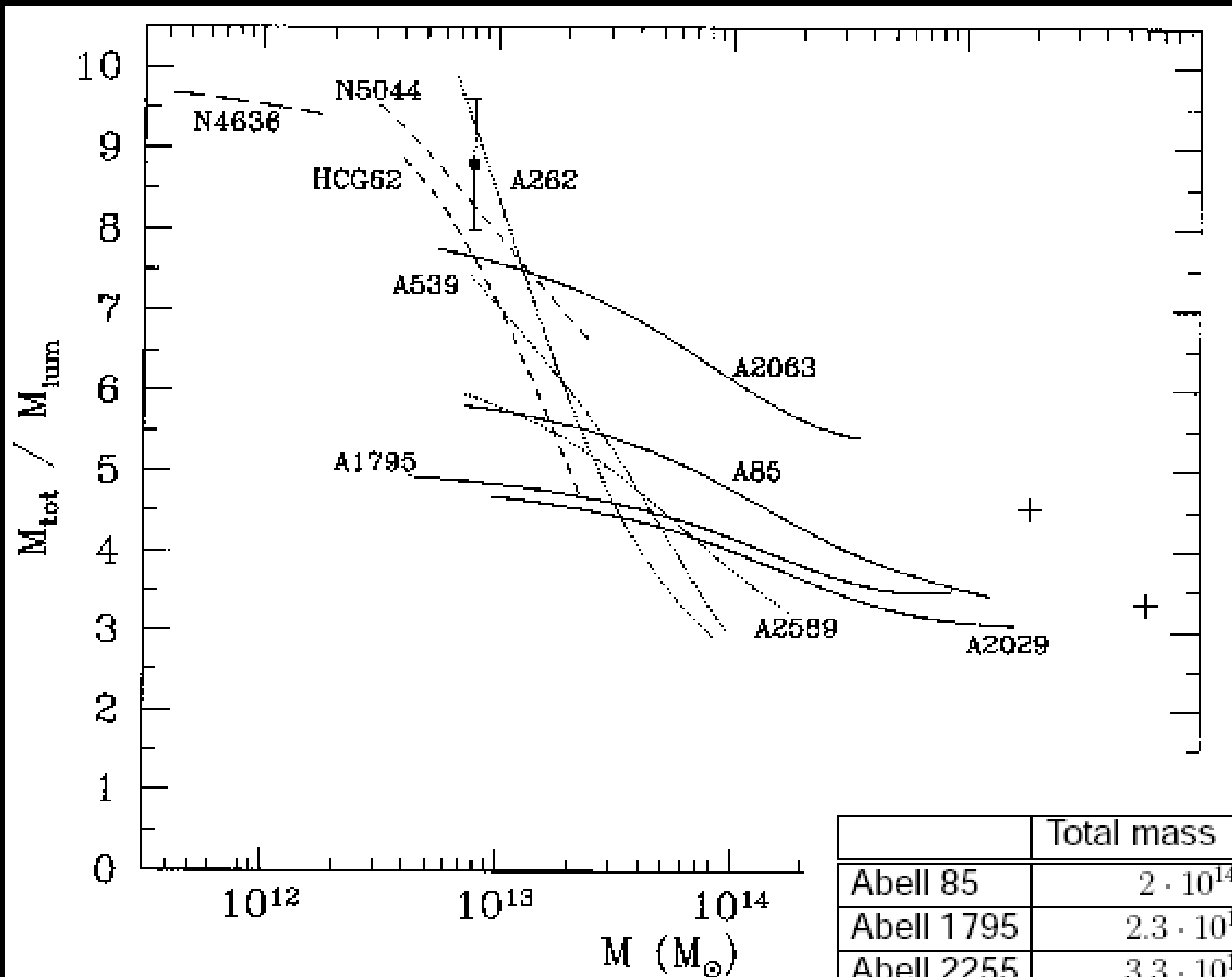

(David, Jones & Forman 1995)

$\rho_{DM} \propto r^{-2}$

$\rho_{gas} \propto r^{-1}$ in groups

$\rho_{gas} \propto r^{-2}$ in richest clusters

Concentration:
Galaxies > DM> hot gas

	Total mass $< 0.5 Mpc$	gas mass $< 0.5 Mpc$
Abell 85	$2 \cdot 10^{14} M_\odot$	$3.4 \cdot 10^{13} M_\odot$
Abell 1795	$2.3 \cdot 10^{14} M_\odot$	$3.6 \cdot 10^{13} M_\odot$
Abell 2255	$3.3 \cdot 10^{14} M_\odot$	$3.5 \cdot 10^{13} M_\odot$
Abell 2256	$6.3 \cdot 10^{14} M_\odot$	$4.1 \cdot 10^{13} M_\odot$

Summary to remember!

- There is hot (10^7 – 10^8 K) low-density (10^{-3} cm^{-3}) intracluster gas with $Z \approx 0.3\text{-}0.4 Z_{\odot}$.
- The gas mass can be estimated through hydrostatic eq.
- The ICG accounts only for 10-20% of the total cluster mass, and it contains more mass than that locked in galaxies.
- There is a Lx - σ relation: richer clusters are brighter
- X-rays are an efficient way to find clusters, but it suffers from cosmological dimming.